Multiple convergences in the evolutionary history of the testate amoeba family Arcellidae (Amoebozoa: Arcellinida: Sphaerothecina): when the ecology rules the morphology

RUBÉN GONZÁLEZ-MIGUÉNS[1,*], CARMEN SOLER-ZAMORA[1], MAR VILLAR-DEPABLO[1,2], MILCHO TODOROV[3] and ENRIQUE LARA[1]

[1]*Real Jardín Botánico (RJB-CSIC), Plaza Murillo 2, 28014 Madrid, Spain*
[2]*Museo Nacional de Ciencias Naturales (MNCN-CSIC), Serrano 115 bis, 28006 Madrid, Spain*
[3]*Institute of Biodiversity and Ecosystem Research, Bulgarian Academy of Science, 1113 Sofia, Bulgaria*

Protists are probably the most species-rich eukaryotes, yet their systematics are inaccurate, leading to an underestimation of their actual diversity. Arcellinida (= lobose testate amoebae) are amoebozoans that build a test (a hard shell) whose shape and composition are taxonomically informative. One of the most successful groups is Arcellidae, a family found worldwide in many freshwater and terrestrial environments where they are indicators of environmental quality. However, the systematics of the family is based on works published nearly a century ago. We re-evaluated the systematics based on single-cell barcoding, morphological and ecological data. Overall, test shape appears to be more related to environmental characteristics than to the species' phylogenetic position. We show several convergences in organisms with similar ecology, some traditionally described species being paraphyletic. Based on conservative traits, we review the synapomorphies of the infraorder Sphaerothecina, compile a list of synonyms and describe a new genus *Galeripora*, with five new combinations. Seven new species: *Arcella guadarramensis* **sp. nov.**, *Galeripora balari* **sp. nov.**, *Galeripora bufonipellita* **sp. nov.**, *Galeripora galeriformis* **sp. nov.**, *Galeripora naiadis* **sp. nov.**, *Galeripora sitiens* **sp. nov.** and *Galeripora succelli* **sp. nov**. are also described here.

ADDITIONAL KEYWORDS: adaptive convergence – convergence – *COI* mtDNA – cryptic species – diversity – phylogeny.

INTRODUCTION

The characterization, classification and delimitation of organisms into basic diversity units like species, is essential in all fields in biology (Mayr, 1944; Wiley, 1978; de Queiroz & Donoghue, 1988; Coyne & Orr, 1989; Wilson, 2017). Indeed, an accurate taxonomy is indispensable for the reproducibility of observations and experiments (Mori *et al.*, 2019). Species delimitation relies on a solid theoretical background, which gave birth to dozens of species concepts (Mayden, 1997; Wheeler & Meier, 2000). The phylogenetic concept of species is probably one of the most widely accepted and defines species as 'the smallest aggregation of populations diagnosable by a unique combination of character states' (Nixon & Wheeler, 1990). While the application of this concept may be challenging in many plants or animals, it becomes even more difficult when it is applied to protists that usually possess fewer diagnostic characters (Schlegel & Meisterfeld, 2003; Boenigk *et al.*, 2012).

Far from being a marginal group in the history of life on Earth, protists occupy all the largest and most ancient clades in the eukaryotic tree, while plants, animals and fungi occupy only lateral branches (Adl *et al.*, 2019). Furthermore, recent work based on environmental DNA sequencing indicates that their diversity may surpass plants and animals (De Vargas *et al.*, 2015; Mahé *et al.*, 2017). Hence, biodiversity studies need to be expanded to protists in order to

obtain a coherent picture of life on Earth. Molecular characterization has been proposed as a way to circumvent issues with identification (Larson, 1998; Zrzavý *et al.*, 1998; Giribet *et al.*, 2002; Casabella-Herrero *et al.*, 2021). However, the lack of a consensus on reference species in many groups renders the use of DNA sequences meaningless as a stand-alone tool for species delimitation. To solve this, an integrative approach grouping ecological, morphological or genetic data appears as the most reasonable strategy (Dayrat, 2005; Padial *et al.*, 2010; Lara *et al.*, 2020).

One of the most charismatic and well-known protists are Arcellinida, a group of Amoebozoa that construct a characteristic shell, or test, which concentrates most features used for their classification (Nikolaev *et al.*, 2005; Gomaa *et al.*, 2017). These organisms are commonly used as bioindicators for ecosystem health (Nguyen-Viet *et al.*, 2007; Patterson *et al.*, 2013; Cockburn *et al.*, 2020; Nasser *et al.*, 2020), and also in palaeoecology to reconstruct ancient climates (Dalby *et al.*, 2000; Mitchell *et al.*, 2008; Qin *et al.*, 2013; Marcisz *et al.*, 2020). Currently, many new taxa are being discovered and described based on the general morphology of their tests (Reczuga *et al.*, 2015; Féres *et al.*, 2016). While this exploration of diversity is essential, molecular studies have revealed that all well-sampled taxa were actually species complexes (Kosakyan *et al.*, 2012), where individual species differed in slight variations of the test shape and size ('pseudocryptic diversity'; Kosakyan *et al.*, 2013; Singer *et al.*, 2015). These 'hidden' species may have different geographical distributions (Heger *et al.*, 2013; Singer *et al.*, 2019) and also occupy different microhabitats (Singer *et al.*, 2018). Pooling these species has, therefore, consequences not only for biodiversity estimates, but also on blurring the bioindication signal (Kosakyan & Lara, 2019).

The new Arcellinida systematics is currently being established through an integrative approach, which combines molecular and morphological data, including scanning electron microscopy observations. It results in the recognition of numerous species characterized by narrower ecological tolerance and more restricted geographical distributions, as compared with the classical systematics built on overall test shape (Lara *et al.*, 2020). Delimiting Arcellinida species can be only achieved using variable molecular markers. In line with this, several authors (Kosakyan *et al.*, 2013, 2016a) have suggested the use of cytochrome *c* oxidase subunit I (*COI*), a mitochondrial marker widely used in zoology (Hebert *et al.*, 2003; Xia *et al.*, 2012; Mas-Peinado *et al.*, 2018), but also in other protists, such as *Cyphoderia* Schlumberger, 1845 (Heger *et al.*, 2011) or the Amoebozoa *Copromyxa* Zopf, 1885 (Kostka *et al.*, 2017) and *Vannella* Bovee, 1965 (Nassonova *et al.*, 2010). Yet, the database on Arcellinida *COI* sequences

still remains poor. Indeed, almost all *COI* data in public databases are from the infraorder Hyalospheniformes (Kosakyan *et al.*, 2012, 2016b), with the exception of two identical sequences from an unidentified species in the genus *Arcella* Ehrenberg, 1830 from *Sphagnum* L. bogs (Fiz-Palacios *et al.*, 2014).

Together with *Antarcella* (Deflandre, 1928), *Arcella* belongs to the family Arcellidae, classified in the infraorder Sphaerothecina. First erected by early protistologist Ehrenberg (1830), the genus *Arcella* initially included three species, with *Arcella vulgaris* Ehrenberg, 1830 as the type species. Later authors, like Cash *et al.* (1919), Greef (1866), Leidy (1876, 1879), Penard (1890, 1902), Playfair (1918) and Wailes (1913), described most species known to date. This information was eventually compiled and reviewed by Deflandre (1928) – this latter work being currently the only most complete reference for the group and is still used today as its most important reference. Deflandre's (1928) study includes a species classification that distributed the species into subgenus *Antarcella*, characterized by a single nucleus and *Euracella* (Deflandre, 1928) with two or more nuclei, respectively. These subgenera were later elevated to genus level and named *Antarcella* and *Arcella*, respectively. The latter was subdivided into four sections based on test outline: 'Vulgares', 'Carinatae', 'Aplanatae' and 'Altae' (Deflandre, 1928).

Arcella is probably the most ecologically successful Arcellinid taxon, found worldwide in environments that range from oligotrophic peatlands to eutrophic and even salt-impacted water bodies (Escobar *et al.*, 2008; Roe & Patterson, 2014; Reczuga *et al.*, 2015; Cockburn *et al.*, 2020). Several species are considered to be cosmopolitan and appear to have extremely broad ecological tolerances, such as, for instance, *Arcella hemisphaerica* Perty, 1852, found from acidic peatlands to coastal salt marshes (Tsyganov & Mazei, 2006; Todorov & Bankov, 2019). These large disparities in species ecologies and geographical distributions suggest, like in other Arcellinida, the existence of a previously overlooked diversity of species to be revealed through integrative taxonomy. It still remains to be evaluated how far the described morphological diversity and systematics is consistent with the species phylogenetic trees.

The aim of this study is to evaluate the current systematics of Arcellidae. We tested the validity of Deflandre's systematic hypotheses (i.e. the validity of the genera *Antarcella* and *Arcella* and the monophyly of the three Western Palaearctic sections in genus *Arcella*). Furthermore, we reveal test morphological diversification patterns in Arcellidae, based on isolates from the Western Palaearctic. For that purpose, we reviewed the bibliography of the original species descriptions within the infraorder Sphaerothecina to re-evaluate putative synapomorphies and to gather

all the information that facilitates further work on the group. Then, we collected individual organisms from a panel of species representing all sections found in the Palaearctic region (i.e. all sections except 'Altae'; Deflandre, 1928). We redefined their taxonomic status based on an integrative taxonomic approach by analysing morphometric, genetic (*COI*) and ecological data inferred from the original habitat.

MATERIAL AND METHODS

Bibliographic search

We carried out an exhaustive search into available published research by compiling all the original species descriptions of the Sphaerothecina infraorder. A synonymic list, together with references to all the original manuscripts, can be found in the Supporting Information (Appendix S1). All corresponding references have been indexed in the bibliography. Each publication was carefully reviewed obtaining the following information, when possible: data on the precise geographic location from where species were described, description of the original ecosystem, test morphology and ornamentation, number of nuclei and images/drawings of the type specimens. We also compared our specimens with Eugène Penard's collection, accessible online (https://commons.wikimedia.org/wiki/Commons:P%C3%A9nard_project/taxon_without_categories, accessed 10 November 2020), an atlas of testate amoebae in Bulgaria (Todorov & Bankov, 2019) and two curated websites containing illustrations of testate amoebae (Siemensma, 2019; Gomes & Souza, 2021).

Sampling and specimen preparation

We sampled environments typical for members of *Arcella*, such as: (1) aquatic: lake and river sediment, among submerged vegetation like *Ceratophyllum* L.; (2) bog: *Sphagnum* mosses; and (3) terrestrial: dry mosses growing on different substrates (Table 1). The countries sampled were Spain, Bulgaria and France. Samples were filtered from the moss and sediment and transferred to a Petri dish to concentrate the testate amoeba tests. The organisms were isolated individually and washed several times in sterile water with a small-diameter pipette, under an inverted microscope. A portion of the cells found were isolated for molecular analyses and deposited individually in Eppendorf tubes containing a guanidine thiocyanate-based nucleic acids extraction buffer (Chomczynski & Sacchi, 1987). Nucleic acids extractions were performed on single cells, as described in Duckert *et al.*, 2018. The other cells were isolated for scanning

electron microscopy (SEM), deposited on stubs and then placed in a desiccator at least overnight prior to metallization and observation.

Microscopical observation

All isolated cells were documented under light microscopy, using a Leica DMI8 inverted microscope, up to 400 × magnification DIC, and a Leica MC170 HD camera with the software Leica application suite (v.4.12.0). The cells were deposited on stubs and coated in 8 nm gold using a Balzers SCD 004 sputter coater and a tension of 15 kV. They were observed with a Hitachi S-3000N and a JEOL JSM-5510 (operating at 10 kV) scanning electron microscope (SEM).

We used the software ImageJ (v.1.52) (Schneider *et al.*, 2012) to obtain accurate test measurements from the images. We measured the aperture length and width, and test length and width to be used later in morphometric analyses.

DNA extraction and amplification

Total DNA was extracted from 46 organisms from the infraorder Sphaerothecina (Kosakyan *et al.*, 2016a), 39 from the genus *Arcella* (family Arcellidae), four from *Cucurbitella* Penard, 1902 and three from *Netzelia* Ogden, 1979 (family Netzeliidae). Members of the last two genera were used as outgroups (Table 1). DNA was extracted from single amoeba cells in guanidine thiocyanate buffer and desalted through several washes in 96% and 70% ethanol dilutions, pelleted and preserved at 4 °C until further processing (Duckert *et al.*, 2018), except on two occasions, where two amoebae were collected together in the same DNA extraction.

The polymerase chain reaction (PCR) consisted of, with occasional minor variations, a final reaction volume of 20 µL containing 6 µL of distilled water, 12 µL MyTaq Red DNA polymerase Mix (BioLine), 1 µL of each primer (10 µmol) and 2 µL of DNA template. We applied a two-step protocol: a first amplification was performed using the universal mitochondrial cytochrome *c* oxidase subunit I (*COI*) primer pair LCO 1490 (5' GGTCAACAAATCATAAAGATATTGG 3') and HCO 2198 (5' TAAACTTCAGGGTGACCAAAAAATCA 3') (Folmer *et al.*, 1994), with the following PCR cycling profile: initial denaturation at 96 °C for 5 min, followed by 40 cycles at 94 °C for 15 s, 40 °C for 15 s and 72 °C for 90 s and a final extension step at 72 °C for 10 min. We designed also two *Arcella*-specific primers, namely ArCOIF (5' GGTATTYTAGCWCATTCNRGTGG 3') and the reverse and complementary ArCOIR, which were applied to the previously obtained products in a semi-nested approach, by combining each of them with

Table 1. Baroded cells with notes on the mitochondrial clade, sampling locations, habitat (Sample type), date of collection and GenBank accessions numbers for cytochrome *c* oxidase subunit I sequences (*COI*), organized following the phylogenetic tree (Fig. 1)

Species, mtDNA clade	Label	Locality	Coordinates	Sample type	Date	GenBank accession
Arcellidae						
Galeripora						
Galeripora sp., A		**United Kingdom**: Dartmoor Forest	50°31'N 3°57'W	**Sphagnum** moss	2010	KJ544163
Galeripora sp., A		**Switzerland:** Amburnex	46°33'N 6°13'E	**Sphagnum** moss	2010	KJ544162
Galeripora succelli, B	R304	**France**: Frasne, La Tourbière	46°49'N 6°9'E	**Sphagnum** moss	2019	MW960372
Galeripora galeriformis, C	C1	**Spain**: Madrid, Rivas-Vaciamadrid	40°19'N 3°30'W	**Terrestrial**: gypsum, dry moss	02/12/2018	MW960395
Galeripora galeriformis, C	C2	**Spain**: Madrid, Rivas-Vaciamadrid	40°19'N 3°30'W	**Terrestrial**: gypsum, dry moss	02/12/2018	MW960394
Galeripora bufonipellita, D	R59	**Spain**: Madrid, San Lorenzo de El Escorial	40°34'N 4°09'W	**Terrestrial**: granite, wet moss	21/10/2018	MW960385
Galeripora bufonipellita, D	R62	**Spain**: Madrid, San Lorenzo de El Escorial	40°34'N 4°09'W	**Terrestrial**: granite, wet moss	21/10/2018	MW960384
Galeripora bufonipellita, D	R180	**Spain**: Madrid, Rascafría	40°51'N 3°56'W	**Terrestrial**: granite, lakeside moss	19/4/2019	MW960379
Galeripora bufonipellita, D	L7	**Spain**: Madrid, Rascafría	40°52'N 3°52'W	**Terrestrial**: granite, wet moss	20/12/2020	MW960389
Galeripora bufonipellita, D	L8	**Spain**: Madrid, Rascafría	40°52'N 3°52'W	**Terrestrial**: granite, wet moss	20/12/2020	MW960388
Galeripora sitiens, E	C4	**Spain**: Castilla La Mancha, Almonacid de Toledo	39°44'N 3°51'W	**Terrestrial**: slate and Quartzite, dry moss	02/12/2018	MW960393
Galeripora sitiens, E	C6	**Spain**: Castilla La Mancha, Almonacid de Toledo	39°44'N 3°51'W	**Terrestrial**: slate and Quartzite, dry moss	02/12/2018	MW960392
Galeripora balari, F	R74	**Spain**: Castilla La Mancha, Cuenca	40°05'N 2°07'W	**Terrestrial**: gypsums, dry moss	19/1/2019	MW960383
Galeripora balari, F	R75	**Spain**: Castilla La Mancha, Cuenca	40°05'N 2°07'W	**Terrestrial**: gypsums, dry moss	19/1/2019	MW960382
Galeripora catinus, G	R309	**France**: Frasne, Le Tourbière	46°49'N 6°9'E	**Sphagnum** moss	2019	MW960371
Galeripora naiadis, H	M243	**Bulgaria**: Sofia, Sofia Southern Park	42°39'N 23°18'E	**Freshwater**: submerged vegetation	31/8/2018	MW960408
Galeripora naiadis, H	M246	**Bulgaria**: Sofia, Sofia Southern Park	42°39'N 23°18'E	**Freshwater**: submerged vegetation	31/8/2018	MW960406
Galeripora naiadis, H	M257	**Bulgaria**: Sofia, Sofia Southern Park	42°39'N 23°18'E	**Freshwater**: submerged vegetation	31/8/2018	MW960402
Galeripora naiadis, H	M247	**Bulgaria**: Sofia, Sofia Southern Park	42°39'N 23°18'E	**Freshwater**: submerged vegetation	31/8/2018	MW960405
Galeripora naiadis, H	M244	**Bulgaria**: Sofia, Sofia Southern Park	42°39'N 23°18'E	**Freshwater**: submerged vegetation	31/8/2018	MW960407
Galeripora naiadis, H	M251	**Bulgaria**: Sofia, Sofia Southern Park	42°39'N 23°18'E	**Freshwater**: submerged vegetation	31/8/2018	MW960404
Galeripora naiadis, H	M252	**Bulgaria**: Sofia, Sofia Southern Park	42°39'N 23°18'E	**Freshwater**: submerged vegetation	31/8/2018	MW960403
Galeripora bathystoma, I	Q2	**Spain**: Madrid, Hoyo de Manzanares	40°35'N 4°55'W	**Freshwater**: submerged vegetation	10/12/2020	MW960387
Galeripora bathystoma, I	Q4	**Spain**: Madrid, Hoyo de Manzanares	40°35'N 4°55'W	**Freshwater**: submerged vegetation	10/12/2020	MW960386
Galeripora polypora, J	A1	**Spain**: Madrid, Aldea del Fresno	40°19'N 4°12'W	**Freshwater**: submerged vegetation	23/11/2020	MW960400
Galeripora polypora, J	A2	**Spain**: Madrid, Aldea del Fresno	40°19'N 4°12'W	**Freshwater**: submerged vegetation	23/11/2020	MW960399
Galeripora polypora, J	R124	**Spain**: Madrid, Aldea del Fresno	40°19'N 4°12'W	**Freshwater**: submerged vegetation	07/4/2019	MW960381
Galeripora polypora, J	R125	**Spain**: Madrid, Aldea del Fresno	40°19'N 4°12'W	**Freshwater**: submerged vegetation	07/4/2019	MW960380
Arcella						
Arcella cf. vulgaris, K	H8	**Spain**: Madrid, Hoyo de Manzanares	40°35'N 4°55'W	**Freshwater**: submerged vegetation	8/12/2020	MW960390
Arcella conica, L	M291	**Bulgaria**: Sofia, Sofia Southern Park	42°39'N 23°18'E	**Freshwater**: submerged vegetation	31/8/2018	MW960401
Arcella cf. vulgaris, M	A5	**Spain**: Madrid, Aldea del Fresno	40°19'N 4°12'W	**Freshwater**: submerged vegetation	23/11/2020	MW960398
Arcella cf. vulgaris, M	A6	**Spain**: Madrid, Aldea del Fresno	40°19'N 4°12'W	**Freshwater**: submerged vegetation	23/11/2020	MW960397
Arcella cf. vulgaris, M	A7	**Spain**: Madrid, Aldea del Fresno	40°19'N 4°12'W	**Freshwater**: submerged vegetation	23/11/2020	MW960396
Arcella guadarramensis, L	R204	**Spain**: Madrid, Puerto de Canencia	40°52'N 3°45'W	**Sphagnum** moss	12/10/2019	MW960378
Arcella guadarramensis, L	R207	**Spain**: Madrid, Puerto de Canencia	40°52'N 3°45'W	**Sphagnum** moss	12/10/2019	MW960377

Table 1. Continued

Species, mtDNA clade	Label	Locality	Coordinates	Sample type	Date	GenBank accession
Arcella guadarramensis, L	R210	**Spain**: Madrid, Puerto de Canencia	40°52′N 3°45′W	***Sphagnum*** moss	12/10/2019	MW960375
Arcella guadarramensis, M	R208	**Spain**: Madrid, Puerto de Canencia	40°52′N 3°45′W	***Sphagnum*** moss	12/10/2019	MW960376
Arcella guadarramensis, M	R211	**Spain**: Madrid, Puerto de Canencia	40°52′N 3°45′W	***Sphagnum*** moss	12/10/2019	MW960374
Arcella guadarramensis, M	R212	**Spain**: Madrid, Puerto de Canencia	40°52′N 3°45′W	***Sphagnum*** moss	12/10/2019	MW960373
Netzeliidae						
Cucurbitella						
Cucurbitella mespiliformis	M30	**Bulgaria**: Sofia, Sofia Southern Park	42°39′N 23°18′E	**Freshwater**: submerged vegetation	15/7/2018	MW960414
Cucurbitella mespiliformis	M32	**Bulgaria**: Sofia, Sofia Southern Park	42°39′N 23°18′E	**Freshwater**: submerged vegetation	15/7/2018	MW960413
Cucurbitella mespiliformis	M37	**Bulgaria**: Sofia, Sofia Southern Park	42°39′N 23°18′E	**Freshwater**: submerged vegetation	15/7/2018	MW960412
Cucurbitella mespiliformis	M41	**Bulgaria**: Sofia, Sofia Southern Park	42°39′N 23°18′E	**Freshwater**: submerged vegetation	15/7/2018	MW960411
Netzelia						
Netzelia lobostoma	M54	**Bulgaria**: Sofia, Sofia Southern Park	42°39′N 23°18′E	**Freshwater**: submerged vegetation	15/7/2018	MW960410
Netzelia lobostoma	M55	**Bulgaria**: Sofia, Sofia Southern Park	42°39′N 23°18′E	**Freshwater**: submerged vegetation	15/7/2018	MW960409
Netzelia lithophila	E2	**Spain**: Madrid, Aldea del Fresno	40°19′N 4°12′W	**Freshwater**: submerged vegetation	4/3/2021	MW960391

the corresponding broad-spectrum primer (respectively, ArCOIR-LCO and ArCOIF-HCO). The PCR profile was the following: initial denaturation at 96 °C for 5 min, followed by 40 cycles at 94 °C for 15 s, 55 °C for 15 s and 72 °C for 90 s, and a final extension step at 72 °C for 10 min. After the amplification, 3 µL of the reaction was analysed by electrophoresis on a 1% agarose gel, to verify fragment size and check for contaminations. Bands with the expected size were excised from the gel and stored at 4 °C. The samples were sequenced using Sanger dideoxy-technology in both directions by the company Macrogen Inc. (Macrogen Europe, Madrid, Spain). The control quality of the raw sequences and the assembling of both PCR products were done using the software GENEIOUS PRIME (v.2019.0.4). Finally, the identity of the sequences was checked by performing a blastn analysis (Altschul *et al.*, 1990) against the GenBank database to ensure that our sequences were the closest related to Arcellinida. The final length of the sequences (from HCO to LCO) was of 641 bp; primers ArCOIR-LCO yielded a 359 bp fragment and ArCOIF-HCO a 259 bp, respectively.

PHYLOGENETIC ANALYSES

We used two *COI* sequences from infraorder Hyalospheniformes: *Hyalosphenia papilio* Leidy, 1874 JN849014 and *Nebela flabellulum* Leidy, 1874 JN849026 (Kosakyan *et al.*, 2012) to root all Sphaerothecina, and added four Lobosea (non-Arcellinida) sequences: *Copromyxa* sp. LC102283, *Copromyxa protea* Fayod, 1883 LC102284, *Hartmannella cantabrigiensis* Zopf, 1885 LC102285 and *Saccamoeba* sp. LC102286 (Kostka *et al.*, 2017) to root all Arcellinida. These sequences were retrieved from GenBank. A total of 52 *COI* sequences were aligned using the MAFFT (Katoh *et al.*, 2002) auto algorithm as implemented in GENEIOUS PRIME (v.2019.0.4), resulting in a total alignment of 618 bp, after removing the primers sequences. A distance table and a neighbour-joining tree (Supporting Information, Fig. S1) were performed with PAUP* v.4.0 b10 (Swofford, 2002) under distance optimality criterion. Tree topologies and node supports were evaluated with Bayesian inferences (BI) and maximum likelihood (ML).

Bayesian inference (BI) analyses were conducted using MrBayes 3.2.7a (Ronquist *et al.*, 2012) implemented in the CIPRES Science Gateway v.3 (Miller *et al.*, 2010). Markov chain Monte Carlo (MCMC) settings consisted of two independent runs, with four chains for each run and 20 10^6 generations. Trees were sampled every 1000 generations; the first 25% was discarded as burn-in. Substitution models were selected with the reversible-jump MCMC method (Huelsenbeck *et al.*, 2004). Posterior probabilities were

calculated with the MCMC method by sampling trees (Larget & Simon, 1999; Huelsenbeck & Ronquist, 2001). Convergence of the different runs was evaluated with TRACER v.1.7.1 (Rambaut *et al.*, 2018), with all the effective sample sizes (ESSs) values over 200. The resulting trees were summarized in a 50% majority rule consensus tree.

Maximum likelihood (ML) analyses were conducted using IQ-TREE (Nguyen *et al.*, 2015). Best substitution models were selected with ModelFinder (Kalyaanamoorthy *et al.*, 2017) under the Bayesian information criterion (BIC). Node supports were assessed with 1000 nonparametric bootstrap replicates. The trees obtained were edited in FigTree v.1.4.3 (Rambaut, 2012).

Morphological analyses

Because we observed a high degree of molecular divergence between sampled populations (Fig. 1; Supporting Information Fig. S1) and a high morphological and molecular homogeneity within populations (see Morphometrics and morphology), data from barcoded and non-barcoded cells from the same population were used for morphological analysis, considering them to be members of the same mitochondrial clade. We measured six continuous traits, test length, test width, aperture length and aperture width in 124 cells from the different morphotypes of *Arcella* encountered (Supporting Information, Table S1). Because the aperture and the test have a round shape, we used mean length and width to avoid possible anomalies in test building, obtaining the variables mean test and aperture diameter that will be used later for morphometric analyses.

Morphological analyses were performed using R software v.3.6.3 (R Core Team, 2013) implemented in RStudio v.1.3.1093 (Rstudio, 2020). We first did an exploratory analysis to check the assumptions of normality and homoscedasticity of the studied variables. The independence of variables was verified by doing an autocorrelation analysis using the package CORRGRAM (Wright, 2017). The variables 'test mean' and 'aperture mean' were used for linear discriminant analysis (LDA), which identifies a combination of morphological traits that could be used for mitochondrial clade delimitation, using the package MASS (Venables & Ripley, 2002). The package ggplot2 (Wickham, 2016) was used to generate a scatterplot.

Taxonomic decisions

To avoid the biases caused by single-gene phylogenies in testing systematic hypotheses (Maddison, 1997),

we used an integrative approach that includes also morphological and ecological information to reconstruct the evolutionary history of the different lineages (Wiley, 1978). The taxonomic decisions that were taken in this study were made once mitochondrial clades were recovered, morphological variation was characterized and analysed, and ecology information was typified. We consider that phylogenetic clades represent independent evolutionary units when, by coalescence processes, they end up depicting concordant clades for mtDNA, morphology and ecology (Kosakyan *et al.*, 2016b; Inoue *et al.*, 2020; Lara *et al.*, 2020; Zhao *et al.*, 2020).

All this information was integrated to re-define the synapomorphies of the different groups within Sphaerothecina (see Taxonomic actions and species accounts). Because type material in Arcellinida usually consists of illustrations (drawings or pictures), we used this type of data to compare our specimens with the described material and to characterize and describe the different species in this study. However, here we deposited one SEM stub per new species at the Royal Botanical Garden of Madrid; these preparations are available under the names MA-Algae11251–11256. The taxonomic decisions were taken in accordance with the rules and recommendations of the International Code of Zoological Nomenclature (ICZN, 1999) which apply to testate amoebae (Lahr *et al.*, 2012).

RESULTS

Molecular phylogeny

Organisms used in the phylogenetic analyses are shown in Table 1. Our phylogenetic analyses recovered the monophyly of Arcellinida with a Bayesian posterior probability (PP) of 1 and a maximum likelihood bootstrap (ML) of 100 (Fig. 1). The infraorder Sphaerothecina was recovered with a PP = 0.99 and a ML = 55, with Arcellidae and Netzeliidae as sister-groups, with a PP = 0.99 and a ML = 37, PP = 0.99 and ML = 66, respectively.

Netzeliidae is composed of four mitochondrial clades. *Netzelia lithophila* (Penard, 1902) appears sister to the clade formed by *Netzelia lobostoma* (Leidy, 1874) and *Cucurbitella mespiliformis* (Penard, 1902) (PP = 0.99 and ML = 92). The latter hosted two mitochondrial clades reciprocally monophyletic (PP = 0.99 and ML = 72).

In Arcellidae we grouped the sequences into mitochondrial clades based on phylogenetic position, named A to O (Fig. 1). The mitochondrial clades K–L are reciprocally monophyletic (PP = 0.91 and ML = 48) and sister to all other mitochondrial clades (PP = 1

and ML = 75). The mitochondrial clade K is sister to the clade formed by L–O (PP = 0.99 and ML = 40), in which M and N–O are reciprocally monophyletic (PP = 1 and ML = 99).

The mitochondrial clades A–F and G–J are reciprocally monophyletic (PP = 1 and ML = 90 and PP = 0.97 and ML = 76, respectively). The reciprocally monophyletic clades A and B (PP = 0.99 and ML = 74) are sister to the clades C–F (PP = 1 and ML = 86), which are composed of two reciprocally monophyletic sister-groups C–D (PP = 0.98 and ML = 54) and E–F (PP = 0.61 and ML = 36). The mitochondrial clade G is sister to the clades H–I (PP = 0.99 and ML = 93), in which H is the sister-group to the reciprocally monophyletic clades I–J (PP = 0.93 and ML = 62).

MORPHOMETRICS AND MORPHOLOGY

The different mitochondrial clades obtained were morphologically classified, based on the qualitative characters of overall test shape, into the different sections defined by Deflandre (1928) (Fig. 1):

- *Section 1, 'Vulgares'*: Hemispherical shape, whose height varies between one-third and four-fifths of the maximum diameter and which do not possess a circular keel (Deflandre, 1928). This includes the mitochondrial clades I, K, M and L identified based on their test outline as: I, *Arcella bathystoma* Deflandre, 1928; K and M, *Arcella cf. vulgaris* Erhenberg, 1830; and L, *Arcella conica* (Playfair, 1918).
- *Section 2, 'Carinatae'*: Morphotypes that look approximately similar to the 'Vulgares' as a ratio height/diameter, but which have a circular test shape that always coincides with the maximum diameter of the keel (Deflandre, 1928). This includes the mitochondrial clades B, C, D, E, F, N and O identified as: B, N and O, *Arcella artocrea* Leidy, 1876; C, D, E and F, *Arcella arenaria* Greef, 1866; and G, *Arcella catinus* Penard, 1890.
- *Section 3, 'Aplanatae'*: Flattened test shape, wide aperture diameter, the ratio of height to diameter generally does not exceed 0.33 and goes down to 0.19 (Deflandre, 1928). This includes here the mitochondrial clades H and J both identified as *Arcella polypora* (Penard, 1902).

The measurements used for the morphometric analysis are shown in the Supporting Information, Table S1. Although the variables used for the morphological analysis only refer to the oral side of the test and, therefore, do not reflect the full morphospace of the different clades, analyses separated efficiently all mitochondrial clades. We only used for morphological analyses those cells for which length and width of the aperture could be measured directly on the pictures (in

total 80 cells); this includes, respectively, ten cells (clade B), four (clade C), four (clade D), three (clade E), 12 (clade F), 21 (clade H), six (clade I), five (clade J), seven (clade L), five (clade N) and three (clade O) (Supporting Information, Table S1) specimens per mitochondrial clade. The oval shape of the clade G, *A. catinus*, could not correctly represent the test diameter, so we exclude this clade for the morphometric analyses.

The linear discriminant analysis (LDA) model is represented in a scatterplot of the scores of linear discriminant functions 1 (LD1) and 2 (LD2) (Fig. 2). This analysis correctly identified the different clades in Arcellidae. The percentages of different linear discriminant axes were 73% for LD1 and 27% for LD2, respectively (Supporting Information, Table S2). Cells were correctly classified within the different mitochondrial clades (100% probability of discrimination) in all cases, except for an overlap between the mitochondrial clades C and F (91%, 11 of 12), both classified as *A. arenaria* in the Deflandre Section 2, and the clades I (66%, 4 of 6) *A. bathystoma* and L (71%, 5 of 7) *A. conica*, both in the Section 1. Also, these two morphological traits (test and aperture diameter), allow a good discrimination of the different sections described by Deflandre (1928) and the different ecologies (Supporting Information, Fig. S2).

DISCUSSION

PHYLOGENETIC POSITION OF ARCELLIDAE AND NETZELIIDAE

Reconstructing the patterns of diversification is essential to understanding the evolutionary history of organisms. In Arcellinida, molecular data allowed unveiling of the deep phylogenetic relationships using conserved molecular markers, usually the nuclear SSU rRNA gene (Lara *et al.*, 2008; Kudryavtsev *et al.*, 2009; Gomaa *et al.*, 2012, 2015, 2017; Lahr *et al.*, 2013; Kosakyan *et al.*, 2016a), *NAD9/NAD7* (Blandenier *et al.*, 2017) and, recently, multigene data obtained from single cells transcriptomes (Lahr *et al.*, 2019). Our phylogenetic trees support the monophyly of Arcellidae Ehrenberg, 1943 and Netzeliidae Kosakyan, Lara *et* Lahr, 2016a as sister-groups forming the infraorder Sphaerothecina Kosakyan *et al.* (2016a), thus confirming previous results with a new molecular marker.

TESTING DEFLANDRE'S SYSTEMATICS HYPOTHESES OF ARCELLIDAE

The nuclei problem, invalidation of genus Antarcella

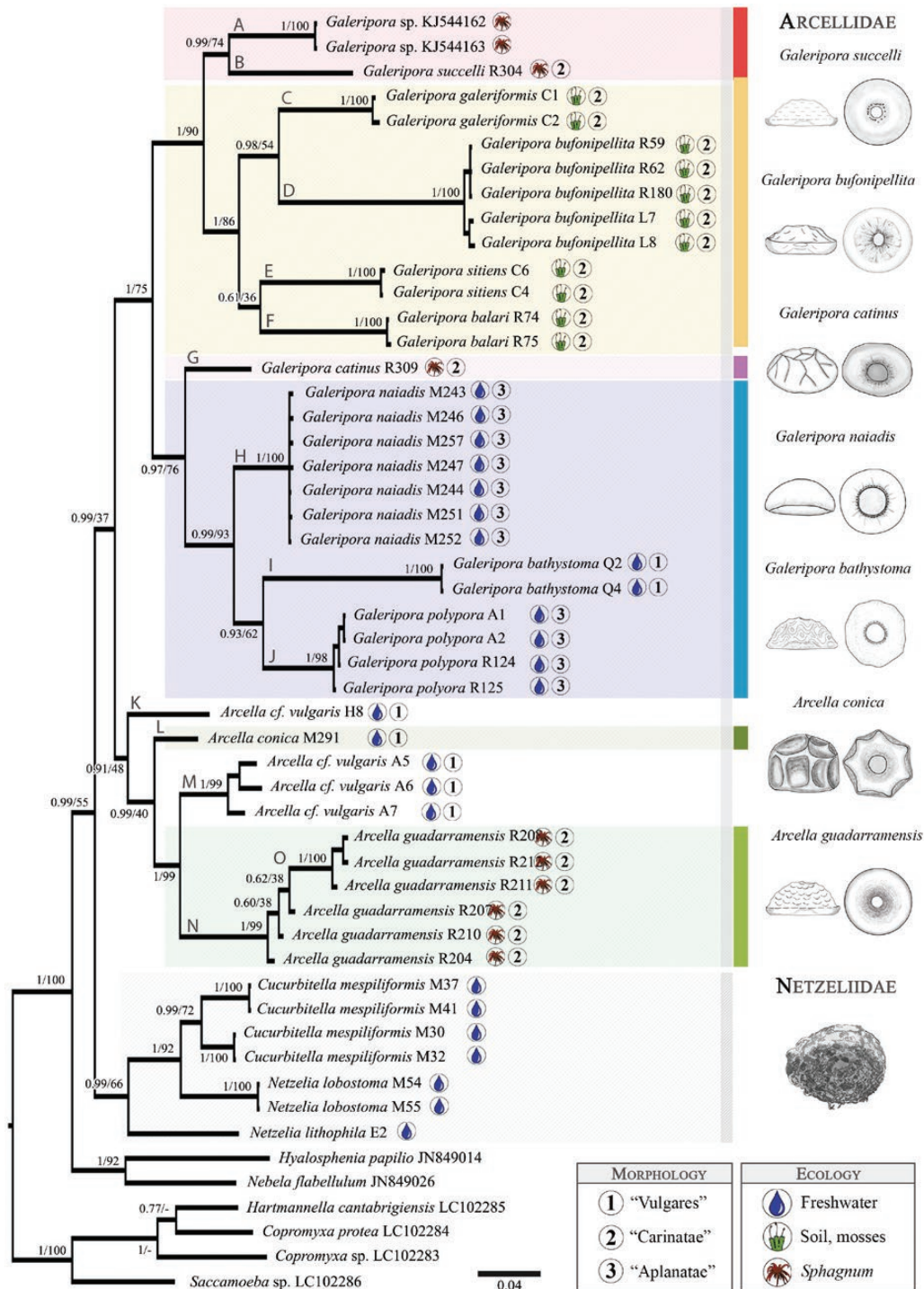Although the systematics of Arcellinida is based almost exclusively on morphological characters of

Figure 1. Bayesian phylogenetic tree based on 52 partial sequences *COI* mtDNA data, 618-nucleotide position alignment. The posterior probability values (Bayesian analysis) and bootstrap values (maximum-likelihood) are represented at each node, with a letter representing the different mitochondrial clades along the branches. The colours represent the mitochondrial clades that compose the different figures. Next to each species name is the original habitat (freshwater/*Sphagnum*/terrestrial mosses) and the section according to Deflandre (1928). The drawings show the tests of illustrative species in lateral and oral side views. Drawings by CSZ.

the test, nuclei have been used occasionally for that purpose (Deflandre, 1928; Ogden & Meisterfeld, 1989). Most Arcellinida only have a single nucleus, except for Arcellidae where higher numbers have been reported, thus playing a role in the systematics of the family.

The first author who highlighted the importance of nuclei number was Collin (1914), who described the uninucleate species *Arcella atava* (Collins, 1914) as a potential sister-group to all other binucleated species of *Arcella*. Indeed, he considered it as a 'representative stage of an ancestral state in *Arcella*' (Collin, 1914), considering the binucleated state as a derived character with respect to possessing a single nucleus. Later, Deflandre (1928) erected the subgenus *Antarcella*, which grouped those species from genus *Arcella* that contain a single nucleus, *A. atava* and *Arcella pseudarcella* (Penard, 1917) and the subgenus *Euarcella* (= *Arcella*), which included the rest of the species, with two or more nuclei. However, this classification has not been followed by subsequent authors, not even by Deflandre himself, who later used solely the morphology of the test to classify and describe new species of *Arcella*, without considering the number of nuclei as a taxonomic character in the systematics of this group. For instance, he synonymized the species *Arcella amphora* (Van Oye, 1926), described with only one nucleus, and *Arcella apicata* (Schaudinn, 1898), based only on test morphology, without considering the number of nuclei (Deflandre, 1928).

Careful observations on nuclei numbers suggest that they may vary within populations. Greef (1866) reported, when describing *Arcella arenaria*, 'In one of the individuals examined, there was only one nucleus'. Hegner (1920) demonstrated that uninucleate specimens appeared in populations of binucleated species. These organisms eventually recovered a binucleated state under culture conditions. Thus, uninucleate cells may simply be a life stage that eventually reverts into a binucleate state later in their complex life-cycle, like those described in the Arcellinida genus *Phryganella* Penard, 1902 (Dumack *et al.*, 2020). Indeed, Mignot & Raĭkov (1992) described for *Arcella vulgaris* a meiotic process where two nuclei degenerated after the first meiotic division and karyogamy occurred later before excystment by fusion of the sister haploid nuclei, thus recovering a uninucleate and diploid state. Hence, being uni- or binucleate varies along a single individual's life cycle, which precludes the use of this criterion in taxonomy. We, therefore, invalidate both subgenera *Euarcella* and *Antarcella*.

Adaptive test morphology, invalidation of Deflandre's sections in Arcella

Deflandre built the systematics of *Arcella* based on overall test morphology, creating four sections (see

Morphometrics and morphology): Section 1 'Vulgares', Section 2 'Carinatae', Section 3 'Aplanatae' and Section 4 'Altae'. From these four sections, only the first three have been reported in the Western Palaearctic; Section 4 'Altae' will not be investigated in this work (Deflandre, 1928). We show through our phylogenetic analysis that none of the proposed sections are monophyletic (Fig. 1). Rather than constituting synapomorphies, the traits that define each section (overall test shape and aperture and test diameter) seem to be related to environmental characteristics (Supporting Information, Fig. S2). Indeed, similar test outlines can be recovered in different branches of the tree but in analogous environments, which represent, most probably, adaptive evolutionary convergences (Fig. 1). Test compression and aperture relative width have been commonly associated to functional traits (Fournier *et al.*, 2012, 2015; Lamentowicz *et al.*, 2020), which corroborates the idea that some test traits at least have an adaptive value. Deflandre (1928) already emphasized the importance of the environment type (in particular water availability) in the assembling of *Arcella* communities.

In aquatic environments all *Arcella* morphotypes could be classified either within Section 1 'Vulgares' (hemispherical test, narrow aperture) or Section 3 'Aplanatae' (flattened test, wide aperture). These findings are in line with earlier works that reported these organisms almost exclusively from aquatic environments worldwide (Playfair, 1918; Deflandre, 1928). In our tree, Section 1 corresponds to the mitochondrial clades I and L, classified as *Arcella bathystoma* and *Arcella conica*, respectively; and Section 3 corresponds to the clades H and J, both classified as *Arcella polypora*. These sections present an independent and unique morphospace (Supporting Information, Fig. S2). Interestingly, these organisms can also have a planktonic behaviour (Schönborn, 1962; Meisterfeld, 1991) and coexist in the water column through the formation of gas bubbles that enable floating (Schönborn, 1962; Cicak *et al.*, 1963; Ogden, 1991). It has been proposed that globular morphology (Section 1) might be favoured in lentic systems, while flattened tests (Section 3) are better represented in lotic environments (Velho *et al.*, 2003; Lansac-Tôha *et al.*, 2014; Arrieira *et al.*, 2016, 2017; Schwind *et al.*, 2016; Marcisz *et al.*, 2020). Accordingly, we found *A. polypora* (clades H and J; Section 3) in the submerged vegetation of a river and in an artificial cascading series of ponds, respectively. In turn, both *A. bathystoma* (clade I) and *A. conica* (clade L), two species with a typical Section 1 morphology, were isolated from lentic ecosystems (ponds). These organisms branched in different parts of the phylogenetic tree (Fig. 1) and may, therefore, represent the result of an evolutionary convergence.
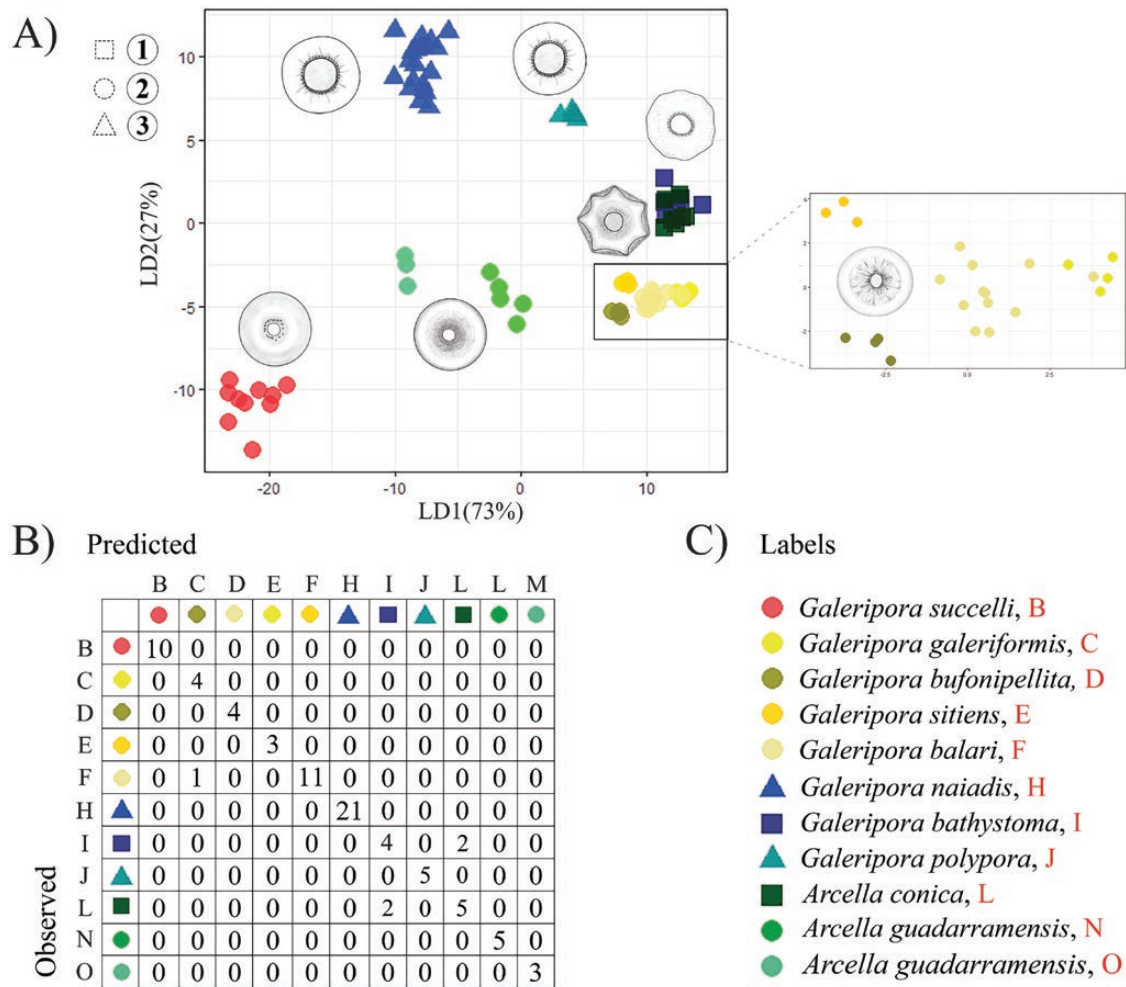
Figure 2. A, scatterplot of the scores of linear discriminants with x-axis representing discriminant function 1 (LD1) and y-axis representing discriminant function 2 (LD2). Colours represent the different mitochondrial clades and symbols refer to the different sections after Deflandre (1928): squares are for Section 1 'Vulgares', circles for Section 2 'Carinatae' and triangles for Section 3 'Aplanatae'. The drawings represent the different morphotypes. B, the table represents the results of a linear discriminant analysis which determines the relationship between predicted and observed specimens cells for each mitochondrial clade.

Similar morphological adaptations can be found in marine planktonic foraminiferans (Birch *et al.*, 2013; Caromel *et al.*, 2014), thus providing more evidence for the adaptive value of the shell.

Sphagnum-dominated peatlands are characterized by the permanent presence of a water film of varying thickness and thus can be considered a subaquatic environment. The common *Arcella* morphologies present in *Sphagnum* are principally recovered in Section 2 'Carinatae'. Here, they are represented by the mitochondrial clades B, N, O (classified as *Arcella artocrea*) and G (*Arcella catinus*). These mitochondrial clades present a unique morphospace in Section 2, with tests resembling Section 1, but with a more flattened

shape and a keel. The mitochondrial clades B and N–O were isolated in analogous environments, in Spain and France, respectively. These clades present similar morphologies and could be classified as *A. artocrea*, but B and N-O occupied a distant position in the phylogenetic tree. The hemispherical shape could be another example of convergent evolution to analogous environments (Figs 1, 3, 8).

Terrestrial environments that are more or less prone to temporal desiccation are represented here by aerial mosses. In these environments, we isolated only members from Section 2 'Carinatae'. Aerial mosses contained members from the mitochondrial clades C–F, resembling *Arcella arenaria*. All these organisms

possess a characteristic flattened test with a narrow aperture; a thin organic layer recovers the test, sealing all pores except those located around the aperture. Here again, the morphology of the test seems to have an adaptive value; flattened tests may have risen as an adaptation to the thin and ephemeral water films in these environments, and the narrow aperture could prevent water loss (Gilbert *et al.*, 2003; Fournier *et al.*, 2015; Koenig *et al.*, 2018). Both traits have been characterized as indicators for xerophilic conditions (Novenko *et al.*, 2016; Tsyganov *et al.*, 2017; Marcisz *et al.*, 2020).

Altogether, overall test outline appears linked to habitats and lifestyles. It is not entirely genetically determined, as a certain degree of phenotypic plasticity has been observed in clonal lineages of *Arcella* concomitantly with environmental changes (Porfírio-Sousa *et al.*, 2017). Here, we show that lineages that live under similar conditions have similar test shapes, independent of their phylogenetic position. This suggests frequent evolutionary adaptive convergences and shows that overall test outline cannot be used as a criterion for genus-level taxonomy in *Arcella*. Therefore, the evolutionary hypothesis behind Deflandre's sections must be rejected, and a new systematics framework for genus *Arcella* must be proposed.

NEW SYSTEMATICS FOR ARCELLIDAE

The combination of *COI* data and SEM documentation has become the silver bullet in Arcellinida species-level systematics, at least in Hyalospheniformes (Kosakyan *et al.*, 2013, 2016b; Singer *et al.*, 2015; Duckert *et al.*, 2018). In *Arcella*, we recovered well-supported mitochondrial clades with members clustering perfectly in the morphometric analyses (Fig. 2). These clades are thus genetically and morphologically coherent. Therefore, we can consider these as genuine biological species following our integrative taxonomic approach (see Taxonomic decisions in Materials and methods).

SUBDIVISIONS IN *ARCELLA* AND ERECTION OF NEW GENUS

While overall test shape has been poorly conserved within lineages, we identified two synapomorphic characters that delimit a robust (PP = 1, ML = 75) group within the genus *Arcella* corresponding to mitochondrial clades A to J (Fig. 1):

- **Character 1**, presence (clades A to J) (Figs 3–6) or absence (clades K to O) (Figs 7, 8) of pores surrounding the test aperture.
- **Character 2**, presence (clades A to J) (Figs 3–6) or absence (clades K to O) (Figs 7, 8) of an organic layer

covering the test. To date, this character has not been used in taxonomy or systematics of *Arcella*, but it is consistent with the molecular phylogeny of the group, and its persistence within clades A to J suggests that it can be considered as a synapomorphy for that group. The organic layer refers to a protein or organic matrix that covers parts of the test, masking the hexagonal building units that compose it.

Based on the good support at the node gathering the last common ancestor of clades A to J in the phylogenetic tree (Fig. 1), and on the systematic retrieval of these test morphological characters in all members of this group, we erect the new genus *Galeripora,* which contains the mitochondrial clades A to J (K to O stay in the genus *Arcella*).

Pseudocryptic diversity and species-level taxonomy

Below we justify the taxonomic treatment of all mitochondrial clades found in this study. The following characters have been considered for species-level taxonomy:

- **Character I**, overall test morphology: although we have shown that this trait cannot be used for deep phylogeny, this trait remains conserved within populations, thus allowing the use of this qualitative character for taxonomic discrimination.
- **Character II**, ornamentation of the test: tests are built of hexagonal units that can vary in size or shape. Tests can also present granulations on the aboral oral side, and the size and number of pores surrounding the aperture aso have a taxonomic value. The use of these qualitative traits allows the discrimination between the closest related species.
- **Character III**, test and aperture diameter: these quantitative characters are constant within the populations, allowing the differentiation of almost all mitochondrial clades (Fig. 2).

GENUS *GALERIPORA*

Mitochondrial clade A is composed of a sequence from an unidentified organism found associated with *Sphagnum* both in Dartmoor Forest (England, UK) and Le Chenit (Jura Mountains, Switzerland) (Fiz-Palacios *et al.*, 2014); the lack of morphological data makes impossible a taxonomic characterization of this mitochondrial clade.

Mitochondrial clade B (Fig. 3) has been found in the French Jura Mountains close to Switzerland (Frasne) in a dry *Sphagnum*-dominated boreal peatbog. It resembles *Arcella artocrea* as described by Leidy (1876) from New Jersey (USA) and all its infraspecific forms and variants: *Arcella artocrea aplanata* described by Grospietsch (1954) from Swedish Lapland, *A. artocrea*
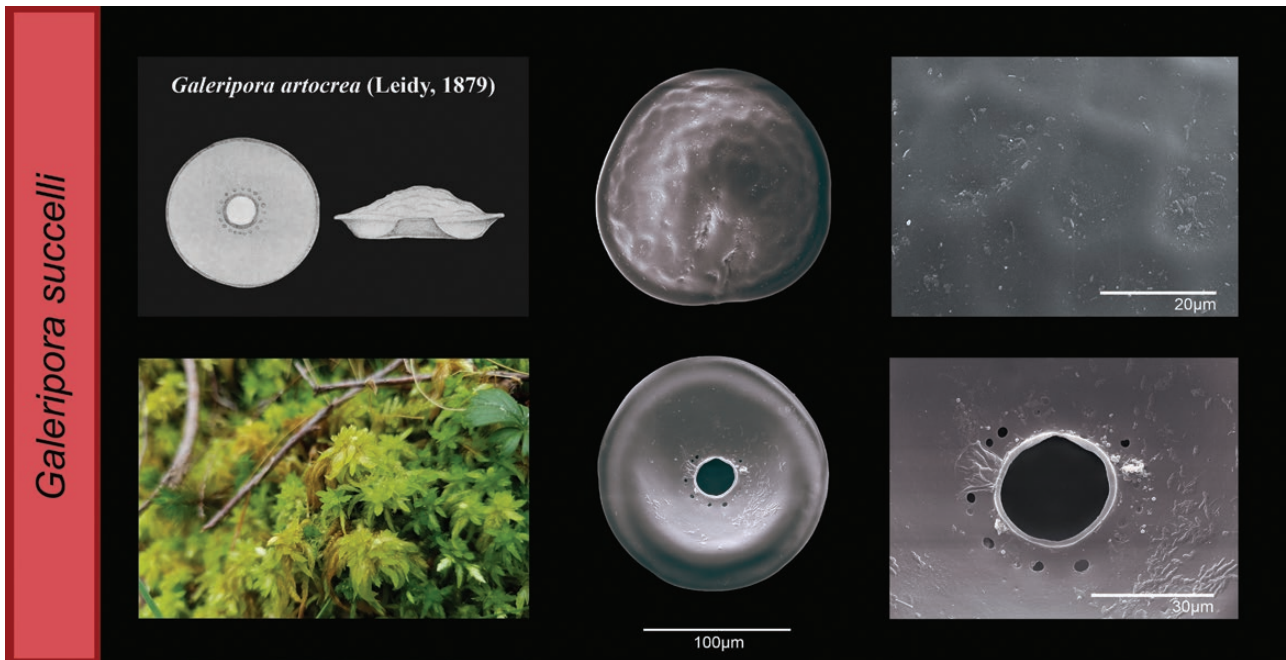
Figure 3. *Galeripora succelli*: scanning electron micrographs of the aboral and oral sides of the test. The images on the right represent a detail of the test and the structure of the aperture. Below left, a photograph of a typical habitat for the species, a peat bog. Above left, original drawing of the closest known resembling species, *Galeripora artocrea* (Leidy, 1879).

catinus Van Oye, 1941 from Krisuvik (Iceland) and *A. artocrea pseudocatinus* Deflandre, 1928 from New Jersey (USA) (Supporting Information, Appendix S1). However, the size of our isolates 173.68–196.57 μm (Supporting Information, Table S1; and see section Taxonomic actions and species accounts) fits better with the description Penard (1902) made for a population from the Swiss Jura Mountains (190–200 μm) than to the organisms described by Leidy (160–176 μm). Penard (1902) already suggested that both populations should be considered as different species, but took no taxonomic action. Based on the proximity of its *terra typica* from Penard's recollection site, we assign a new name to this population: *Galeripora succelli*, as a separate taxon from the American population described by Leidy (1879), which remains *Galeripora artocrea* (Leidy, 1876).

Mitochondrial clades C, D, E and F (Fig. 4) together form a clade and share similar morphology and ecology. These clades resemble the species *Arcella arenaria* Greef, 1866, described from Bonn, Germany. However, *A. arenaria* has a test diameter of 100 μm, a size not reached by any of our isolates. For this reason, we consider that they must represent still unnamed independent species. Test ultrastructure alone can be used to discriminate between clades C and F versus D and E (Fig. 4). Furthermore, each individual clade

can be differentiated based on morphometry of the test and aperture diameter (Fig. 2). These clades present a relatively high molecular divergence between them (Supporting Information, Fig. S1), although the organisms were collected within a geographically limited area in the centre of the Iberian Peninsula (Clade C–D 60 km, C–E 70 km, C–F 120 km, D–E 100 km, D–F 180 km, E–F 150 km). We retrieved clade D in three different years (2018, 2019 and 2021) at the same locality, suggesting the existence of a stable population. Habitats differ also drastically, as clades C and F were found on mosses growing on gypsum (i.e. typically pH > 8.5), while clades D and E were found in granite and quartzite zones, respectively (i.e. typically pH < 6.5). It has been shown that selection or adaptation to microhabitats can structure the communities and drive the evolution of closely related species (Ehleringer & Cooper, 1988; Martin, 1998; Marshall *et al.*, 2016; Mas-Peinado *et al.*, 2018). In Arcellinida, it has been shown that microhabitats harbour different communities of pseudocryptic species (Singer *et al.*, 2018). Therefore, *Galeripora arenaria*, as the species has been delimited until now, has to be considered as a complex of species. For all these reasons, we describe each of these clades as new species: clade C as *Galeripora galeriformis*, clade D as *Galeripora bufonipellita*, clade E as *Galeripora sitiens* and clade F as *Galeripora balari*.
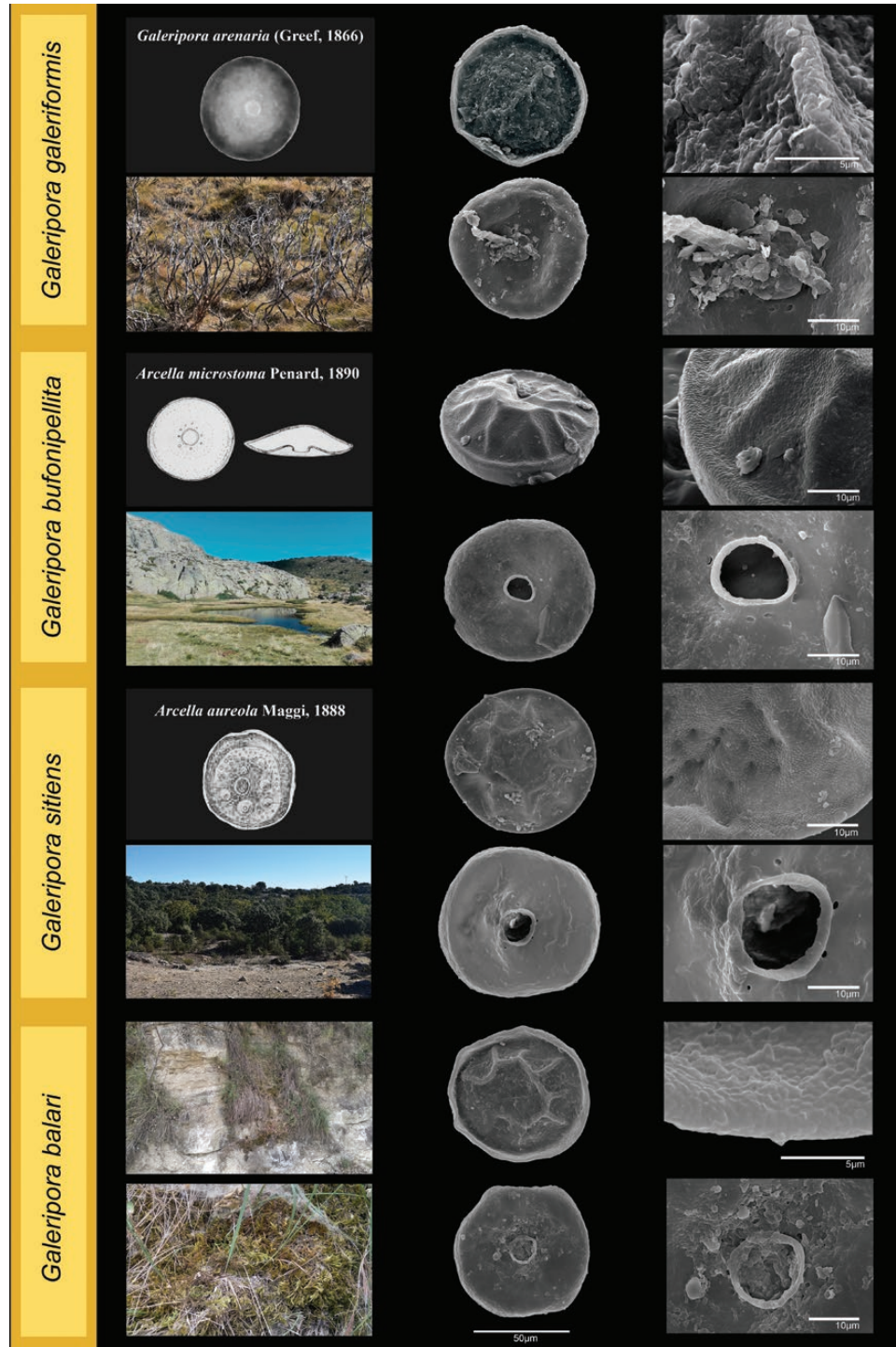
Figure 4. *Galeripora galeriformis*, *Galeripora bufonipellita*, *Galeripora sitiens* and *Galeripora balari*: scanning electron micrographs of the aboral and oral sides of the test. The images on the right represent detail of the test and the structure of the aperture. On the left, a photograph of a typical habitat for each species, original drawing of the closest resembling species *Galeripora arenaria* (Greef, 1866), and original drawings of the synonymized species *Arcella microstoma* Penard, 1890 and *Arcella aureola* Maggi, 1888.
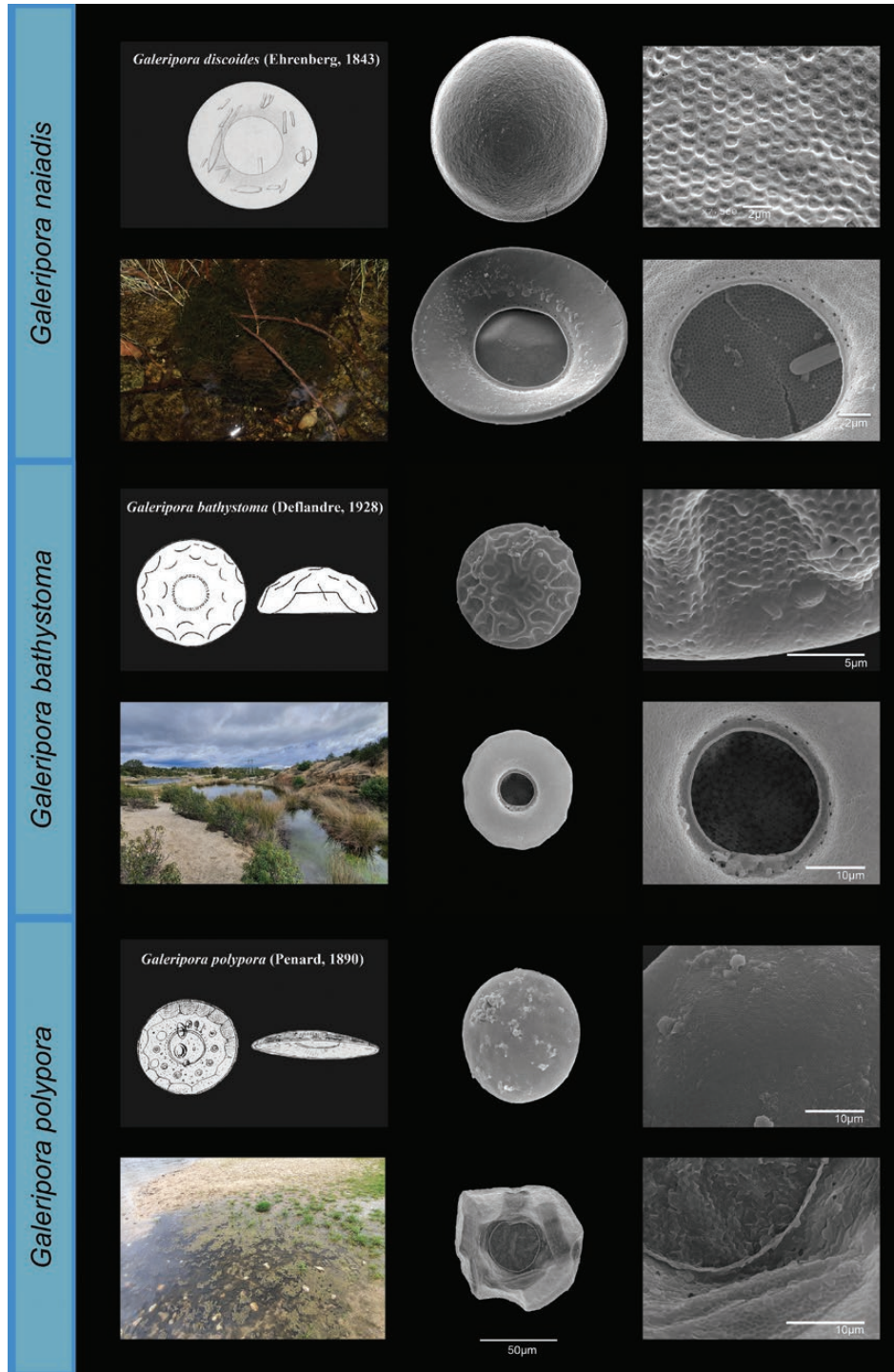
Figure 5. *Galeripora naiadis*, *Galeripora bathystoma* and *Galeripora polypora*: scanning electron micrographs of the aboral and oral sides of the test, for *G. naiadis* the images correspond with pictures of *Arcella discoides* in Todorov & Bankov (2019). The images on the right represent a detail of the test and the structure of the aperture. On the left, a photograph of a typical habitat for each species, original drawing of the closest resembling species *Galeripora discoides* (Ehrenberg, 1843), and original drawing of *Galeripora bathystoma* (Deflandre, 1928) and *Galeripora polypora* (Penard, 1890).
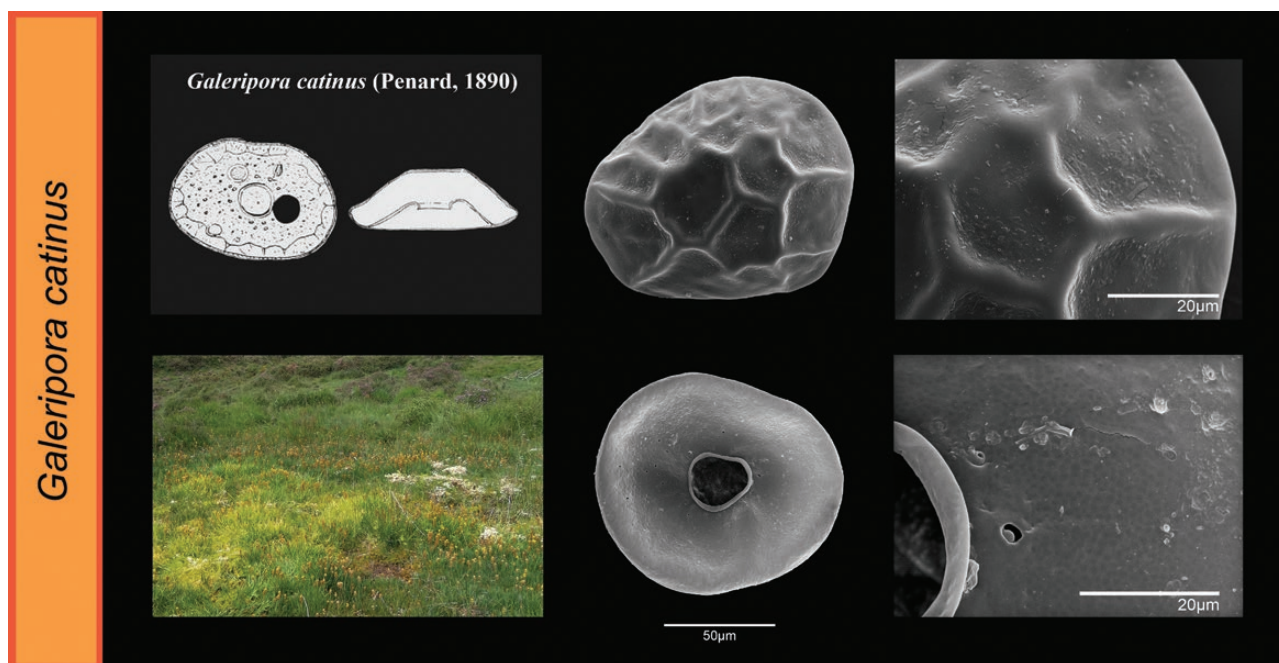
Figure 6. *Galeripora catinus*: scanning electron micrographs of the aboral and oral sides of the test. The images on the right represent a detail of the test and the structure of the aperture. On the left, a photograph of a typical habitat for the species, a peat bog and original drawing of *Galeripora catinus* (Penard, 1890).

Mitochondrial clade G has been isolated from Frasne (France), from *Sphagnum* moss. The cells recorded in this clade can be morphologically assignable to *Arcella catinus* Penard, 1890, based on the test shape in the original drawings and on test diameter (original description 122 µm; clade G 74.4–79.6 µm). The *terra typica* given by Penard (1890) when describing *A. catinus* is Wiesbaden (Germany) located *c*. 400 km from Frasne, a reasonable range for testate amoeba species (Singer *et al.*, 2019). The habitat (*Sphagnum* hummock in a peat bog) also corresponds. Nonetheless, the large size given by Penard in his original description suggests the existence of a species complex behind *Galeripora catinus*.

Mitochondrial clades H and J have a typical morphology for Deflandre Section 3 ('Aplanatae'). Clade H has been recovered in Bulgaria (Sofia), and its test dimensions do not correspond with any known members of Section 3; we named clade H as *Galeripora naiadis*. On the other hand, clade J from the river Alberche near Madrid (Spain) was morphologically assignable to *Arcella polypora* (original description 80–120 µm; clade J 99.6–114.5 µm), notably larger than the typical *Galeripora discoides* (original description 81 µm) and we, therefore, kept the name *Galeripora polypora*. We retrieved this species in two consecutive years (2019–20) suggesting that the species forms stable populations in its original sampling site.

Mitochondrial clade I forms a robust clade in our tree with *G. naiadis* and *G. polypora*. Its morphology fits perfectly with *Arcella bathystoma* Deflandre, 1928, as both test shape and dimensions fit with the original description (original description 55–62 µm; clade I, 68.6–79.2). This aquatic species was collected in granitic permanent ponds in Spain, near Hoyo de Manzanares (Community of Madrid). We refer to this mitochondrial clade as *Galeripora bathystoma*.

GENUS *ARCELLA*

Mitochondrial clades N and O share an almost identical test outline with *Galeripora succelli*, but are both notably smaller. Both clades can be differentiated molecularly (Fig. 1) and morphologically (Fig. 2). However, we decided here to follow a conservative approach, because we consider that further sampling is required to demonstrate a discontinuity before separating both clades into different taxonomic units. Therefore, we pool both N and O clades into a single taxonomic unit. They have been found together in the same location, small *Sphagnum* hummocks in a fen located on the Canencia Pass (Community of Madrid, Spain). We named this new species *Arcella guadarramensis*.

Mitochondrial clade L is composed of only one sequence, morphologically assignable to *Arcella conica* (Playfair, 1918), based on the original drawings and also on the measurements (original description 50–80 µm;
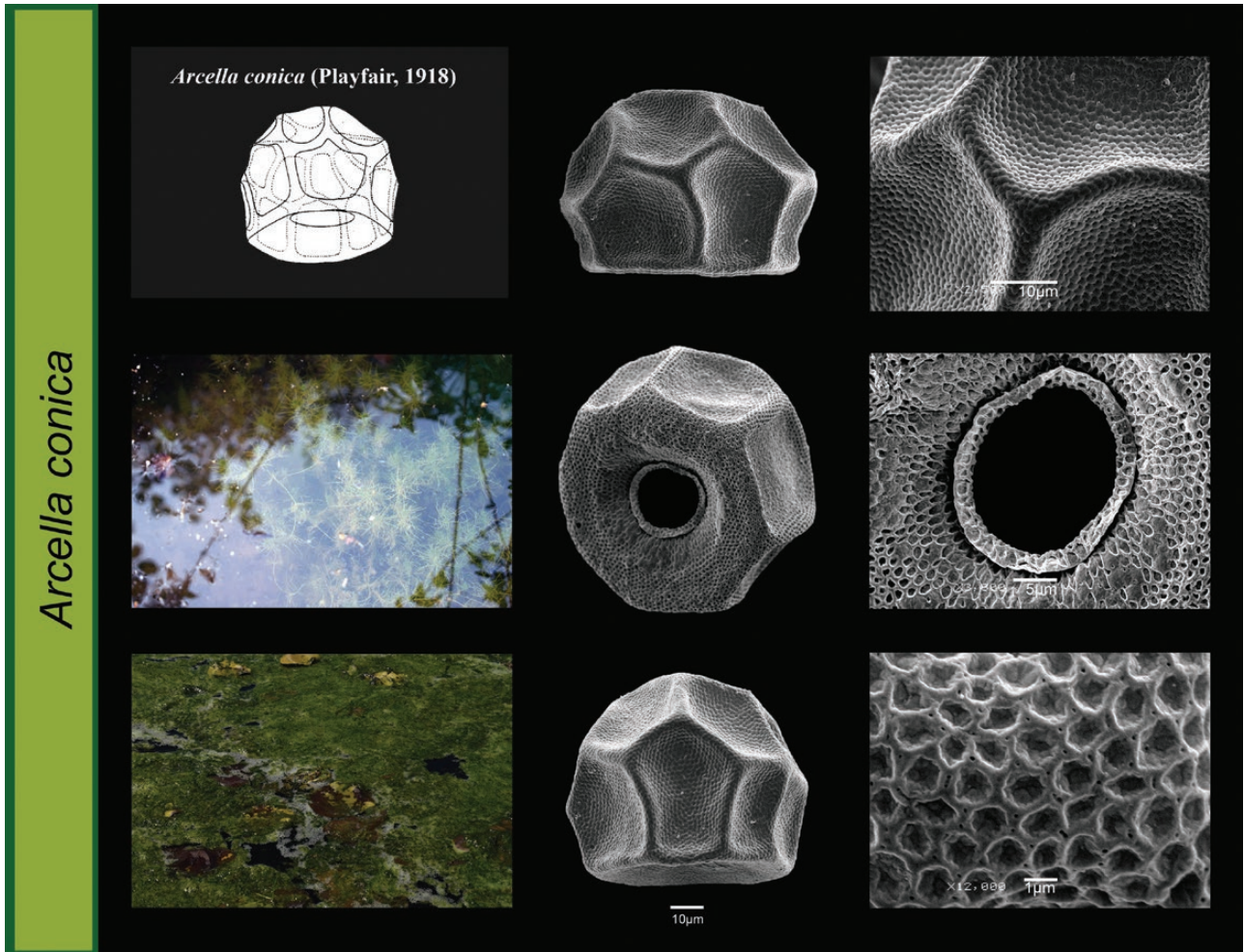
Figure 7. *Arcella conica*: scanning electron micrographs of the aboral, oral and lateral sides of the test. The images on the right represent a detail of the test and the structure of the aperture. On the left, photographs of a typical habitat for the species, and original drawing of *Arcella conica* (Playfair, 1918).

clade L 73.1–79.3 µm). *Arcella conica* was described from Auburn, Lismore and Woodlawn (Australia); given the tendency for restricted geographical distributions observed in testate amoeba species, and especially the importance of the Tropic of Cancer desert belt as a separation between austral and boreal faunas in testate amoebae (Smith & Wilkinson, 2007), it seems unlikely that our European isolates from Bulgaria (Sofia) might belong to the same species that Playfair observed. Sampling and isolating Australian cells, and a detailed study of the ultrastructure of all isolates, may clarify the true identity of the isolated organisms. Before more information is made available, we keep this lineage as *Arcella conica*.

Mitochondrial clades K and M are composed of sequences recovered in lentic and lotic freshwater ecosystems, respectively, in Spain. These mitochondrial clades were classified as *Arcella vulgaris* based on the overall test morphology, but we did not obtain enough individuals to proceed to morphometric analyses and, therefore, we have refrained from making any taxonomic decision on these organisms.

Our investigation on the diversity of the genus *Arcella* has revealed a high degree of pseudocryptic diversity, comparable to what has been observed in the other Arcellinida genera *Nebela* and *Hyalosphenia* (Hyalospheniformes) (Heger *et al.*, 2013; Kosakyan *et al.*, 2013). Also, in line with the latter, pseudocryptic species have been found in habitats that differ fundamentally in parameters important for protists such as relative humidity and pH (Bates *et al.*, 2013), which suggests different ecological ranges. Further investigation, including other habitats and regions in the world, will probably reveal a wealth of new diversity in *Arcella*, shedding light on the phylogenetic relationships between phylogroups.
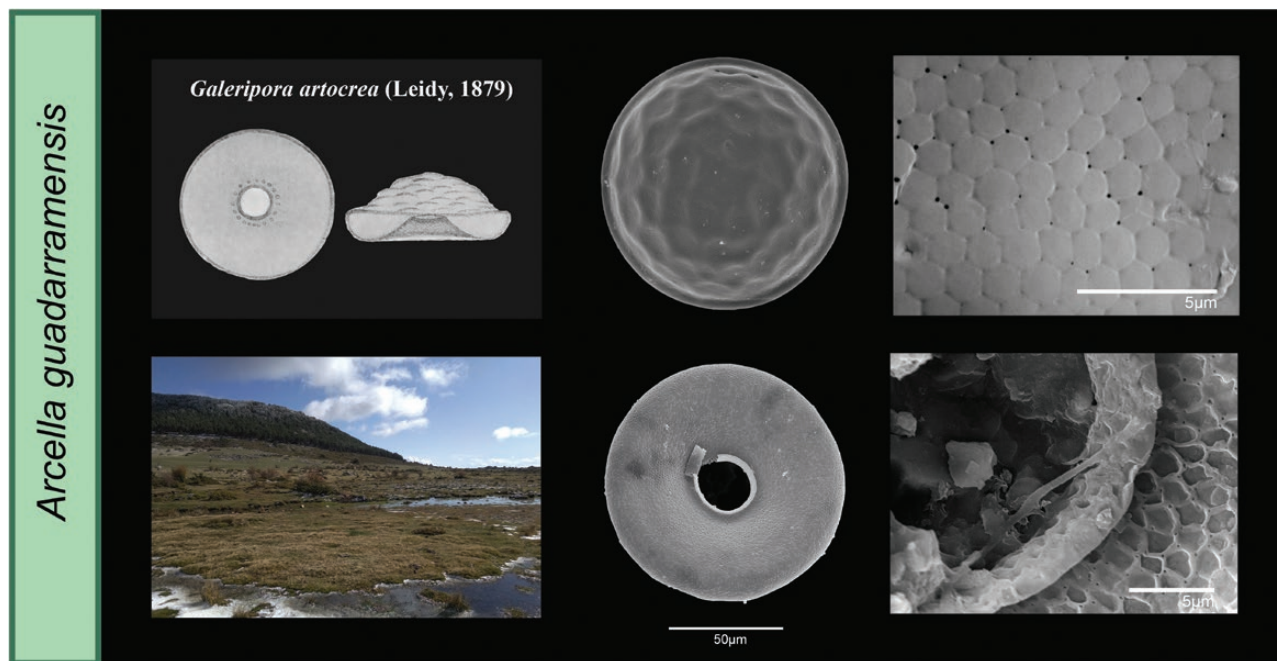
Figure 8. *Arcella guadarramensis*: scanning electron micrographs of the aboral and oral sides of the test. The images on the right represent a detail of the test and the structure of the aperture. On the left, a photograph of a typical habitat for this species, and original drawing of the closest resembling species, *Galeripora artocrea* (Leidy, 1879).

TAXONOMIC ACTIONS AND SPECIES ACCOUNTS

ORDER ARCELLINIDA KENT, 1880

SUBORDER GLUTINOCONCHA LAHR *ET AL.*, 2019

INFRAORDER SPHAEROTHECINA KOSAKYAN *ET AL.*, 2016

Updated diagnosis: Tests have a central aperture, are rounded and have a radial symmetry in cross-section. Most have the capacity to build their own test without foreign material, possibly with self-secreted components.

Type family: Netzeliidae.

Included taxa: (Supporting Information, Appendix S1).

FAMILY NETZELIIDAE KOSAKYAN *ET AL.*, 2016

Type species: Netzelia oviformis (Cash, 1909).

Updated diagnosis: Globular or oviform tests, with radial symmetry. Aperture is central, regular or lobed and forms a collar towards the outside of the test. Presence of irregular, 'nail'-shaped idiosomes or/and exogenous materials, when these are available.

Included taxa: (Supporting Information, Appendix S1).

Difflugia lobostoma Leidy, 1874 and *Difflugia lithophila* Penard, 1902 share many traits with members of the genus *Netzelia*, such as *Netzelia achlora* (Penard, 1902), *Netzelia gramen* (Penard, 1902) and *Netzelia oviformis* (Cash, 1909), placed in the genus *Netzelia* by Gomaa *et al.* (2017). The main reason for the similarity between these species was the capacity to build a test with idiosomes independently from the presence of building material (Ogden, 1979). Later works showed that *Difflugia lobostoma* also had this ability, justifying its inclusion within the genus *Netzelia* (Medioli *et al.*, 1987). Furthermore, both *D. lobostoma* and *D. lithophila* have planktonic life-stages, like many Sphaerothecina. *Cucurbitella* in turn, has been included into Sphaerothecina (Lahr *et al.*, 2019) based on its round/oval-shaped test and the presence of a collar around the aperture, but classified as *incertae sedis*. Nevertheless, this genus shares with the genus *Netzelia* the ability of building a test without incorporating foreign particles (Medioli *et al.*, 1987). Our phylogenetic tree shows (Fig. 1) that *D. lithophila*, *D. lobostoma* and *Cucurbitella mespiliformis* form a clade sister to the family Arcellidae, therefore we include the genus *Cucurbitella* with the family Netzeliidae and transfer *D. lithophila* and *D. lobostoma* to the genus *Netzelia* (see Supporting Information, Appendix S1).

Differential diagnosis between genera: Cucurbitella differs from *Netzelia* as the development of its collar
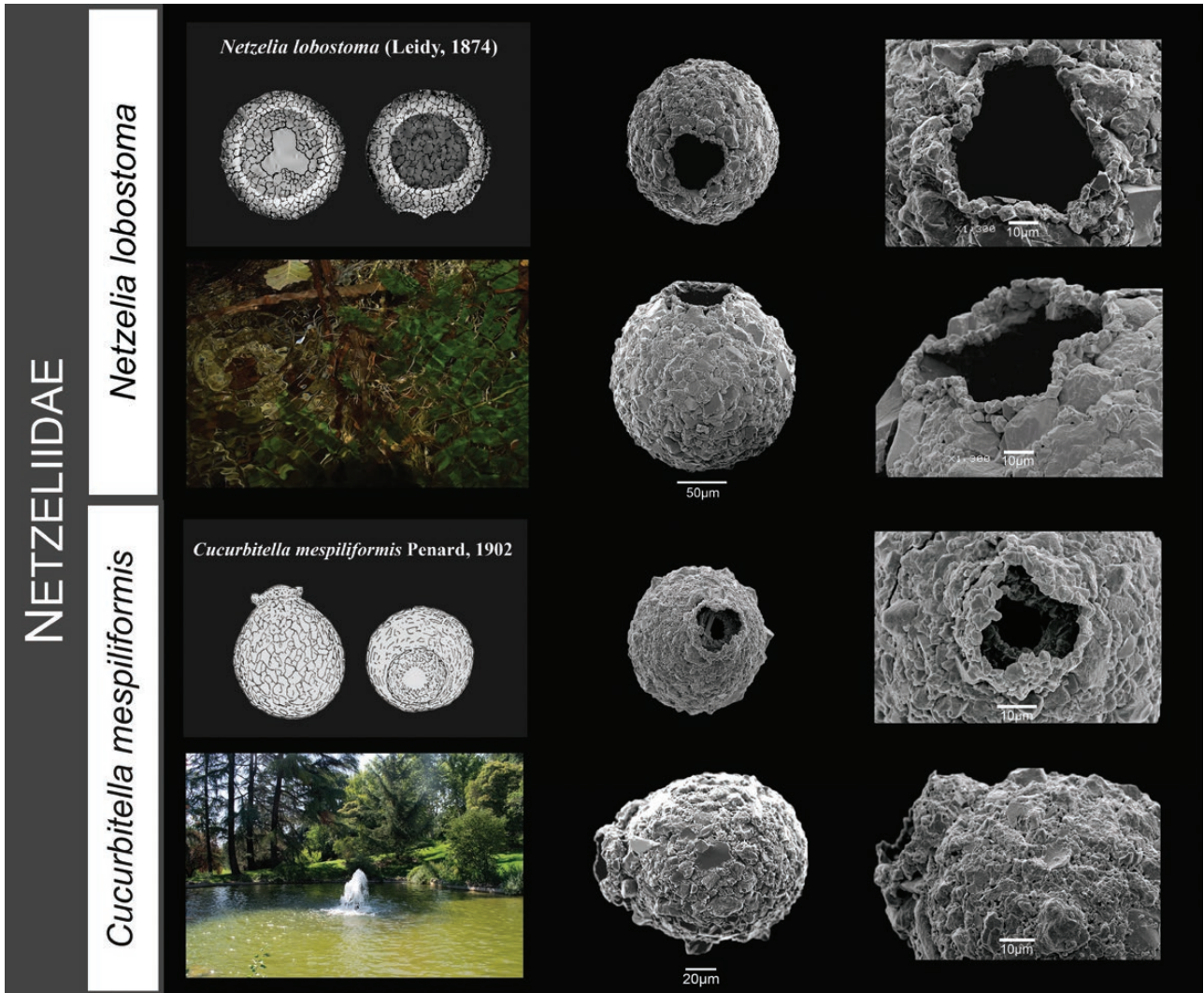
Figure 9. *Netzelia lobostoma* and *Cucurbitella mespiliformis*: scanning electron micrographs of oral and lateral view of the test. The images on the right represent details of the collar. On the left, a photograph of a typical habitat for these species, and original drawings of *Netzelia lobostoma* (Leidy, 1874) and of *Cucurbitella mespiliformis* (Penard, 1902).

creates an internal diaphragm, forming a second chamber with a central aperture (Fig. 9).

NETZELIA LITHOPHILA (PENARD, 1902) **COMB. NOV**.

Difflugia hydrostatica var. *lithophila* Penard, 1902.
Zoobank registration: urn:lsid:zoobank. org:act:4968EA2D-6C2B-417B-AD2B-762E2723018A.

NETZELIA LOBOSTOMA (LEIDY, 1874) **COMB. NOV**.

Difflugia proteiformis Lamarck, 1816: 95.
Cucurbitella tricuspis–Carter, 1856: 221; Medioli *et al.*, 1987.

Difflugia tricuspis Carter, 1856: 221.
Difflugia lobostoma Leidy, 1874: 79.
Zoobank registration: urn:lsid:zoobank. org:act:0AD69577-89AD-42E8-9C40-03A68C73EFD4.

FAMILY ARCELLIDAE EHRENBERG, 1843

Type species: Arcella vulgaris Ehrenberg, 1830.

Included taxa: (Supporting Information, Appendix S1).

Differential diagnosis between genera: (see Discussion).

GENUS ***GALERIPORA*** GONZÁLEZ-MIGUÉNS,
SOLER-ZAMORA, VILLAR-DEPABLO, TODOROV & LARA
GEN. NOV.

Zoobank registration: urn:lsid:zoobank.org:act: 73C0B8C8-FFA4-48CC-8AE5-B0266D983995.

Type species: Galeripora sitiens González-Miguéns, Soler-Zamora, Villar-dePablo, Todorov & Lara

Description: Tests built exclusively with proteinaceous organic material. Shape more or less campanulate, with a central and circular aperture and radial symmetry. The aperture is surrounded by pores. The ultrastructure of the test is composed of hexagonal units that are at least partially covered with an organic matrix layer. Commonly, two or more nuclei, situated at opposite sides of the cytoplasm.

Derivatio nominis: The name is derived from the Latin *galerus*, helmet and '-*porī*', translated as 'helmet-pores'. This name suggests the general shape of the theca that forms the members of this group, and the pores surrounding the opening, one of the synapomorphies of this genus.

Included taxa: Galeripora arenaria, *G. balari*, *G. bathystoma*, *G. bufonipellita*, *G. catinus*, *G. discoides*, *G. galeriformis*, *G. naiadis*, *G. polypora*, *G. sitiens* and *G. succelli*.

GALERIPORA SUCCELLI GONZÁLEZ-MIGUÉNS &
LARA, **SP. NOV**.

(FIG. 3)

Zoobank registration: urn:lsid:zoobank.org:act: 097341BF-C706-47DD-AB62-0467FC280DCB.

Holotype: MA-Algae11252.

Specific diagnosis: Test diameter 180.06–200.14 µm, average of 187.77 µm (*N* = 19); aperture 24.37–33.35 µm, average 29.56 µm (*N* = 10). Colour ranges from transparent to yellow-orange. Subhemispherical test shape, with flattened edges and dimples in the surface that gives the test a golf-ball shape.

The aboral side presents no ribs or keels. Building units are covered with an organic matrix that prevents observation of the building units, giving a smooth outlook to the test. The oral side is also flat and smooth, covered with an organic matrix that prevents observation of the test building units, with a central aperture. The only pores at the base of the test are localized around the aperture, following a circular pattern and curling slightly outwards to form a small ring or lip.

Intraspecific variability: The number of pores surrounding the aperture can be variable. There may be certain deformations in the test that prevent it from having a perfectly circular morphology.

Diagnosis with closely related species: Galeripora succelli can be diagnosed by its specific sequences of the mtDNA markers and by its phylogenetic placement. *Galeripora succelli* differs from *Arcella guadarramensis* by (1) its morphometric differences (see Morphometrics and morphology; Fig. 2) and it is larger than *A. guadarramensis* (see above); (2) a regular and marked granulation on the top of the test; and (3) the absence of pores along the edge of the arboral side of the test.

Habitat: Wet *Sphagnum* moss, in a bog.

Type locality: France, Frasne, La Tourbière (46°49'N 6°9'E).

Etymology: The name is derived from the Gaulish god Succellos (-or *Succellus*, in its latinized form). '*Cellos*' meaning striker and the prefix '*su*' good, the god's name could, therefore, be translated as 'the Good Striker'. As god of agriculture, forests and traditional medicine, he was believed to be in charge of keeping the soil fertile. We propose this name in referring to the type locality being a fertile place with a great abundance of vegetation and surrounded by many crops.

GALERIPORA GALERIFORMIS GONZÁLEZ-MIGUÉNS,
SOLER-ZAMORA, VILLAR-DEPABLO, TODOROV & LARA,
SP. NOV.

(FIG. 4)

Zoobank registration: urn:lsid:zoobank.org:act:09628A92-07D4-4DA7-BF68-A803B3A9D5D5.

Holotype: MA-Algae11253.

Specific diagnosis: Test diameter: 71.65–74.95 µm, average 73.20 µm (*N* = 4); aperture 11.15 to 12.10 µm average 11.50 µm (*N* = 4). Colour ranges from transparent to yellow-orange. General test shape is rounded and flattened.

The aboral side of the test has a small elevation at the top that gives the test a helmet shape; the surface does not have pores and presents a granular pattern of irregular shape. Large ridges cross the aboral side of the test. The oral side of the test is smooth, covered

with an organic matrix that prevents the observation of test building units, with a central aperture. Pores are localized on the brim of the oral side and around the aperture, following a circular pattern. The aperture is invaginated outwards forming a short ring or lip.

Intraspecific variability: The shape and number of ridges on the aboral side of the test can be variable. The number of pores around the aperture is variable. There may be certain deformations in the test that prevent it from having a perfectly circular morphology.

Diagnosis with closely related species: Galeripora galeriformis can be diagnosed by its specific sequences of the mtDNA markers and by its phylogenetic placement (see Molecular phylogeny; Fig. 1). Differs morphologically from other species closely related to *Galeripora arenaria* by presenting (1) morphometric differences (see Morphometrics and morphology; Fig. 2), with a smaller test and aperture diameters than all species presented here; (2) pores along the edge of the base test; (3) presence of a dome in the top part of the test; and (4) irregular granulations of the top surface of the test.

Habitat: Moss on dry gypsum; terrestrial.

Type locality: Spain, Madrid, Rivas-Vaciamadrid, near Laguna del Campillo (40°19'N 3°30'W).

Etymology: The name is derived from the Latin *galerus*, helmet, and *forma*, shape. We propose this name because a Roman helmet is round and wide with a flat brim, similar to the test of this species.

GALERIPORA BUFONIPELLITA GONZÁLEZ-MIGUÉNS & LARA, **SP. NOV**.
(FIG. 4)

Zoobank registration: urn:lsid:zoobank. org:act:8262B0F0-8E1B-48E4-902D-DB867DC0D5BE.

Holotype: MA-Algae11254.

Specific diagnosis: Test diameter: 89.05–92.95 µm, average 90.35 µm (*N* = 8); aperture 13.45–17.85 µm, average 14 µm (*N* = 4). Colour ranges from transparent to yellow-orange. General test shape is rounded and flattened.

The aboral side of the test has several ridges that elevate the test forming a dome and flap borders; the surface does not have pores and presents a granular pattern of regular shape. The oral side of the test is smooth, covered with an organic matrix that prevents

the observation of test building units, with a central aperture. Pores are localized only around the aperture, following a circular pattern and curling slightly outwards to form a small ring or lip. The aperture is invaginated outwards forming a short ring or lip.

Intraspecific variability: The shape and number of ridges on the aboral side of the test can be variable. The number of pores around the aperture is variable. There may be certain deformations in the test that prevent it from having a perfectly circular morphology.

Diagnosis with closely related species: Galeripora bufonipellita can be diagnosed by its specific sequences of the mtDNA markers and by its phylogenetic placement. Differs morphologically from *Galeripora arenaria* closely related species by (1) morphometric differences (see Morphometrics and morphology; Fig. 2); (2) the absence of pores along the edge of the aboral side of the test; and (3) a regular and marked granulation in the top surface of the test.

Habitat: Mosses on the edge of a lake, partially (and temporally) submerged, growing on granitic rocks.

Type locality: Spain, Madrid, Rascafría (40°51'N 3°56'W) and (40°52'N 3°52'W) and San Lorenzo de El Escorial (40°34'N 4°09'W).

Etymology: The name is derived from the Latin *bufo*, toad and *pellis*, animal skin. We propose this name because of the ornamentation of the aboral side of the test, which is reminiscent of the warty skin of a toad.

GALERIPORA SITIENS GONZÁLEZ-MIGUÉNS, SOLER-ZAMORA, VILLAR-DEPABLO, TODOROV & LARA, **SP. NOV**.
(FIG. 4)

Zoobank registration: urn:lsid:zoobank. org:act:02BD3509-F96A-4EA0-8131-03DC5DD5BA6B.

Holotype: MA-Algae11255.

Specific diagnosis: Test diameter: 86.50–92.65 µm, average 88.89 µm (*N* = 8); aperture 16.20–16.85 µm, average 16.60 µm (*N* = 3). Colour ranges from transparent to yellow-orange. General test shape is rounded and flattened.

The aboral side of the test has several ridges that elevate the test forming a dome and flap borders; the surface does not have pores and presents a granular pattern of regular shape. The oral side of the test is smooth, covered with an organic matrix that

prevents observation of the test building units, with a central aperture. Pores are localized only around the aperture, following a circular pattern. The aperture is invaginated outwards forming a short ring or lip.

Intraspecific variability: The shape and number of ridges on the aboral side of the test can be variable. The number of pores around the aperture is variable. There may be certain deformations in the test that prevent it from having a perfectly circular morphology.

Diagnosis with closely related species: Galeripora sitiens can be diagnosed by its specific sequences of the mtDNA markers and by its phylogenetic placement. Differs morphologically from *Galeripora arenaria* and closely related species by (1) morphometric differences (see Morphometrics and morphology; (Fig. 2); (2) the absence of pores along the edge of the aboral side of the test; and (3) a regular granulation of the top surface of the test.

Habitat: Moss on dry slate and quartzite terrestrial.
Type locality: Spain, Castilla La Mancha, Almonacid de Toledo (39°44'N 3°51'W).

Etymology: The name is derived from the Latin *sitiens*, dry or thirsty. We propose this name because the habitat of this species is characterized by prolonged drought with episodic rainfall.

GALERIPORA BALARI GONZÁLEZ-MIGUÉNS & LARA, SP. NOV.

(FIG. 4)

Zoobank registration: urn:lsid:zoobank. org:act:8000271F-3AAD-4EBE-898B-29AB8908D5E2.

Holotype: MA-Algae11256.

Specific diagnosis: Test diameter: 72.95–84.20 µm, average 79.69 µm ($N = 22$); aperture 11.50–14.15 µm average 12.92 µm ($N = 12$). Colour ranges from transparent to yellow-orange. General test shape is rounded and flattened.

The aboral side of the test has a small elevation at the top that gives the test a hat shape; presence of several ridges elevate the test forming a dome and flap borders; the surface does not have pores and presents a granular pattern of irregular shape. The oral side of the test is smooth, covered with an organic matrix that prevents observation of the test building units, with a central aperture. Pores are localized on the brim of the oral side and around the aperture, following a circular pattern and curling slightly outwards to form a small ring or lip. The aperture is evaginated outwards forming a short ring or lip.

Intraspecific variability: The shape and number of ridges on the aboral side of the test can be variable. The number of pores around the aperture is variable. There may be certain deformations in the test that prevent it from having a perfectly circular morphology.

Diagnosis with closely related species: Galeripora balari can be diagnosed by its specific sequences of the mtDNA markers and by its phylogenetic placement (see Molecular phylogeny; Fig. 1). Differs morphologically from other *Galeripora arenaria* closely related species by presenting (1) morphometric differences (see Morphometrics and morphology; Fig. 2); (2) small pores along the edge of the base test; and (3) irregular and marked granulations of the top surface of the test.

Habitat: Mosses overhanging from a rock, in dry gypsum terrestrial.

Type locality: Spain, Castilla La Mancha, Cuenca (40°05'N 2°07'W).

Etymology: The name is derived from the Irish Celtic mythology '*Balar*', which means 'the flashing one'. Balar, a Fomorian leader, was described as a giant with a large eye that causes destruction when opened. He has been inferred as an incarnation of drought, plague and burning sun. We propose this name because the morphology of this species is similar to that of an eye, and because the type locality is a dry area.

GALERIPORA NAIADIS GONZÁLEZ-MIGUÉNS, SOLER-ZAMORA, VILLAR-DEPABLO, TODOROV & LARA, SP. NOV.

(FIG. 5)

Zoobank registration: urn:lsid:zoobank. org:act:A6005873-8045-40E2-B0E1-DE073A2EC66B.

Specific diagnosis: Test diameter 139.20–153.80 µm, average of 146.78 µm ($N = 21$); aperture 48.70–59.10 µm, average 53.76 µm ($N = 21$). Colour ranges from transparent to yellow-orange. The test has a discoid, flattened shape. The edges of the test are somehow curved, giving the whole test a concave outlook, like a bowl.

The aboral side of the test is flat. Building units can be partially covered with a proteinaceous matrix preventing the observation of these units. When this proteinaceous matrix is absent, small pores can be observed at the vertices of the building units, which are then located on both the aboral and oral sides. The oral side presents an aperture invaginated outwards forming a short ring or lip surrounded by many small pores.

Intraspecific variability: The number of pores at the base of the test and the degree of coverage by the organic matrix can be variable. There may be certain deformations in the test that prevent it from having a perfectly circular morphology.

Differences: Galeripora naiadis can be diagnosed by its specific sequences of the mtDNA markers and by its phylogenetic placement. Differs morphologically from other species closely related to *Galeripora polypora* by presenting (1) morphometric differences (see Morphometrics and morphology; Fig. 2) and (2) by its concave outlook.

Habitat: Submerged vegetation, *Ceratophyllum submersum*, in an artificial lake.

Type locality: Bulgaria: Sofia, Sofia Southern Park (42°39'N 23°18'E).

Etymology: The name is derived from the Greek Ναϊάδες, the Naiads, who were female spirits or nymphs who ruled the rivers in Ancient Greek mythology. We propose this name to refer to the ecology of this species – pristine freshwater environments.

GALERIPORA ARENARIA (GREEF, 1866) COMB. NOV.
(FIG. 4)

Arcella aureola Maggi, 1888.
Arcella microstoma Penard, 1890.
Zoobank registration: urn:lsid:zoobank. org:act:C1404AAE-CD5B-4825-9B47-F746BBF4E007.

GALERIPORA ARTOCREA (LEIDY, 1876) COMB. NOV.
(FIGS 3, 8)

Zoobank registration: urn:lsid:zoobank.org:act: 19035B9C-B9FA-481E-AE0A-532695FEEDD3.

GALERIPORA BATHYSTOMA (DEFLANDRE, 1928) COMB. NOV.
(FIG. 5)

Zoobank registration: urn:lsid:zoobank. org:act:71B87508-D89E-4DD6-88DD-BA74DBDB3303.

GALERIPORA CATINUS (PENARD, 1890) COMB. NOV.
(FIG. 6)

Arcella catinus var. australis Playfair, 1918.
Arcella vulgaris var. compressa Cash, 1905.
Zoobank registration: urn:lsid:zoobank. org:act:4E606BBB-DB09-4125-8FE8-579064E97E08.

GALERIPORA DISCOIDES (EHRENBERG, 1843) COMB. NOV.
(FIG. 5)

Arcella homeochlamys discoides Ehrenberg, 1871.
Zoobank registration: urn:lsid:zoobank. org:act:A9EB4B63-6D14-451F-89BA-A37A5C146883.

GALERIPORA POLYPORA (PENARD, 1890) COMB. NOV.
(FIG. 5)

Zoobank registration: urn:lsid:zoobank. org:act:77A12E43-4702-4BBD-B26A-F1E2A093955F.

GENUS ARCELLA EHRENBERG, 1830

Type species: Arcella vulgaris Ehrenberg, 1830.

Included taxa: (Supporting Information, Appendix S1).

ARCELLA GUADARRAMENSIS GONZÁLEZ-MIGUÉNS & LARA, SP. NOV.
(FIG. 8)

Zoobank registration: urn:lsid:zoobank. org:act:57A3452C-3C46-44F2-A5C9-48496E34BB57.

Holotype: MA-Algae11251.

Specific diagnosis: Test diameter: clade L: 114.60–125.90 µm, average 120.30 µm (*N* = 6); aperture 19.60–30.00 µm, average 23.63 µm. clade M 141.50–149.95 µm, average 146.06 µm (*N* = 4); aperture 31.25–34.50 µm, average 33.08 µm. Besides a difference in size, both clades have an identical morphology. Colour ranges from transparent to yellow-orange. Subhemispherical test shape, with flattened edges and dimples in the surface that gives the test a golf ball shape. No ribs or keels on the aboral side. Hexagonal building units are visible, which gives the test a rough appearance; little pores can be seen at the vertices. Building units can also be appreciated at the oral side of the test, with pores at the vertices and a central aperture. The aperture is invaginated outwards forming a short ring or lip.

Intraspecific variability: The building units may vary slightly in shape. Some building units may be collapsed, giving a rough surface. There may be certain deformations in the test that prevent it from having a perfectly circular morphology.

Diagnosis with closely related species: Arcella guadarramensis can be diagnosed by its specific sequences

of the mtDNA markers and by its phylogenetic placement. *Arcella guadarramensis* differs morphologically from similar-looking *G. succelli* by (1) its morphometric differences with *G. succelli* (see Morphometrics and morphology; Fig. 2), both, clade N and O, are notably smaller than *G. succelli* and (2) the rough outlook of the test.

Habitat: Wet *Sphagnum* moss, in a fen.

Type locality: Spain, Madrid, Puerto de Canencia (40°52'N 3°45'W).

Etymology: The name is derived from River Guadarrama, a river with a name of Arabic roots: *wadi*, river, and *ar-rama*, sandy. We propose this name as a reference to the type locality in 'Sierra de Guadarrama', a mountain range named after this river.

We provide a key (Supporting Information, Table S3) and a new figure (Supporting Information, Fig. S3) to facilitate the identification of the new species.

CONCLUSION

Our analyses showed that overall the test outline is not a good criterion for deep phylogeny in Arcellidae, because test compression appears more closely linked to the type of environments that the organisms live in, than to phylogenetic relationships. The adaptive value of test morphology is supported by the fact that species living in similar environments may have the same overall shape, but be distantly related, like *Galeripora succelli* and *Arcella guadarramensis*. Given that Deflandre's (1928) classification was based on overall test shape, it must be updated. Our phylogenetic analyses suggest that the presence of pores surrounding the aperture and of an organic layer on the test are traits that are conserved enough to be used for the delimitation of major groups in Arcellinida. Based on this conclusion, we erect the new genus *Galeripora* to accommodate all species that possess these characters. In addition, we reveal another instance of pseudocryptic diversity in Arcellinida, i.e. species with a similar appearance that can be differentiated based on morphometrics and/ or test ornamentation patterns. These closely related species may differ in their ecological requirements, as suggested by their different original habitats. Based on these conclusions, we proposed five new combinations: *Galeripora arenaria*, *G. bathystoma*, *G. catinus*, *G. discoides* and *G. polypora,* and seven new

species: *Arcella guadarramensis*, *Galeripora balari*, *G. bufonipellita*, *G. galeriformis*, *G. naiadis*, *G. sitiens* and *G. succelli*.

DATA AVAILABILITY

The data underlying this article are available in GenBank Nucleotide Database at https://www.ncbi. nlm.nih.gov/genbank/, and can be accessed with the accession number MW960371-MW960414.

REFERENCES

Adl SM, **Bass D**, **Lane CE**, **Lukeš J**, **Schoch CL**, **Smirnov A**, **Agatha S**, **Berney C**, **Brown MW**, **Burki F**, **Cárdenas P**, **Čepička I**, **Chistyakova L**, **Campo J**, **Dunthorn M**, **Edvardsen B**, **Eglit Y**, **Guillou L**, **Hampl V**, **Heiss AA**, **Hoppenrath M**, **James TY**, **Karnkowska A**, **Karpov S**, **Kim E**, **Kolisko M**, **Kudryavtsev A**, **Lahr DJG**, **Lara E**, **Le Gall L**, **Lynn DH**, **Mann DG**, **Massana R**, **Mitchell EAD**, **Morrow C**, **Park JS**, **Pawlowski JW**, **Powell MJ**, **Richter DJ**, **Rueckert S**, **Shadwick L**, **Shimano S**, **Spiegel FW**, **Torruella G**, **Youssef N**, **Zlatogursky V**, **Zhang Q. 2019.** Revisions to the classification, nomenclature, and diversity of eukaryotes. *Journal of Eukaryotic Microbiology* **66:** 4–119.

Altschul SF, **Gish W**, **Miller W**, **Myers EW**, **Lipman DJ. 1990.** Basic local alignment search tool. *Journal of Molecular Biology* **215:** 403–410.

Arrieira RL, **Schwind LTF**, **Joko CY**, **Alves GM**, **Velho LFM**, **Lansac-Tôha FA. 2016.** Relationships between environmental conditions and the morphological variability of planktonic testate amoeba in four neotropical floodplains. *European Journal of Protistology* **56:** 180–190.

Arrieira RL, **Schwind LTF**, **Bonecker CC**, **Lansac-Tôha FA. 2017.** Temporal dynamics and environmental predictors on the structure of planktonic testate amoebae community in four neotropical floodplains. *Journal of Freshwater Ecology* **32:** 35–47.

Bates ST, **Clemente JC**, **Flores GE**, **Walters WA**, **Parfrey LW**, **Knight R**, **Fierer N. 2013.** Global biogeography of highly diverse protistan communities in soil. *ISME Journal* **7:** 652–659.

Birch H, **Coxall HK**, **Pearson PN**, **Kroon D**, **O'Regan M. 2013.** Planktonic foraminifera stable isotopes and water column structure: disentangling ecological signals. *Marine Micropaleontology* **101:** 127–145.

Blandenier Q, **Lara E**, **Mitchell EAD**, **Alcantara DMC**, **Siemensma FJ**, **Todorov M**, **Lahr DJG. 2017.** NAD9/NAD7 (mitochondrial nicotinamide adenine dinucleotide dehydrogenase gene) – a new 'Holy Grail' phylogenetic and DNA-barcoding marker for Arcellinida (Amoebozoa)? *European Journal of Protistology* **58:** 175–186.

Boenigk J, **Ereshefsky M**, **Hoef-Emden K**, **Mallet J**, **Bass D. 2012.** Concepts in protistology: Species definitions and boundaries. *European Journal of Protistology* **48:** 96–102.

Caromel AGM, **Schmidt DN**, **Phillips JC**, **Rayfield EJ. 2014.** Hydrodynamic constraints on the evolution and ecology of planktic foraminifera. *Marine Micropaleontology* **106:** 69–78.

Carter HJ. 1856. Notes on the freshwater Infusoria of the island of Bombay. *Annals and Magazine of Natural History Ser. 2* **18:** 221–249.

Casabella-Herrero G, **Martínez-Ríos M**, **Viljamaa-Dirks S**, **Martín-Torrijos L**, **Diéguez-Uribeondo J. 2021.** Aphanomyces astaci mtDNA: insights into the pathogen's differentiation and its genetic diversity from other closely related oomycetes. *Fungal Biology* **125:** 316–325.

Chomczynski P, **Sacchi N. 1987.** Single-step method of rna isolation by acid guanidinium thiocyanate–phenol–chloroform extraction. *Analytical Biochemistry* **162:** 156–159.

Cicak A, **McLaughlin JJA**, **Wittenberg JB. 1963.** Oxygen in the gas vacuole of the rhizopod protozoan, *Arcella*. *Nature* **199:** 983–985.

Cockburn CF, **Gregory BRB**, **Nasser NA**, **Patterson RT. 2020.** Intra-lake Arcellinida (testate lobose amoebae) response to winter de-icing contamination in an eastern Canada road-side 'Salt Belt' lake. *Microbial Ecology* **80:** 366–383.

Collin B. 1914. Notes protistologiques. *Archives de Zoologie Expérimentale et Générale* **54:** 85–97.

Coyne JA, **Orr HA. 1989.** Patterns of speciation in *Drosophila*. *Evolution* **43:** 362–381.

Dalby AP, **Kumar A**, **Moore JM**, **Patterson RT. 2000.** Utility of arcellaceans (thecamoebians) as paleolimnological indicators in tropical settings: Lake Sentani, Irian Jaya, Indonesia. *Journal of Foraminiferal Research* **30:** 135–142.

Dayrat B. 2005. Towards integrative taxonomy. *Biological Journal of the Linnean Society* **85:** 407–417.

Deflandre G. 1928. Le genre Arcella Ehrenberg. *Archiv für Protistenkunde* **64:** 152–287.

Duckert C, **Blandenier Q**, **Kupferschmid FAL**, **Kosakyan A**, **Mitchell EAD**, **Lara E**, **Singer D. 2018.** En garde! Redefinition of *Nebela militaris* (Arcellinida, Hyalospheniidae) and erection of *Alabasta* gen. nov. *European Journal of Protistology* **66:** 156–165.

Dumack K, **Görzen D**, **González-Miguéns R**, **Siemensma F**, **Lahr DJG**, **Lara E**, **Bonkowski M. 2020.** Molecular investigation of *Phryganella acropodia* Hertwig et Lesser, 1874 (Arcellinida, Amoebozoa). *European Journal of Protistology* **75:** 125707.

Ehleringer JR, **Cooper TA. 1988.** Correlations between carbon isotope ratio and microhabitat in desert plants. *Oecologia* **76:** 562–566

Escobar J, **Brenner M**, **Whitmore TJ**, **Kenney WF**, **Curtis JH. 2008.** Ecology of testate amoebae (thecamoebians) in subtropical Florida lakes. *Journal of Paleolimnology* **40:** 715–731.

Féres JC, **Porfírio-Sousa AL**, **Ribeiro GM**, **Rocha GM**, **Sterza JM**, **Souza MBG**, **Soares CEA**, **Lahr DJG. 2016.** Morphological and morphometric description of a novel shelled amoeba *Arcella gandalfi* sp. nov. (Amoebozoa:Arcellinida) from Brazilian continental waters. *Acta Protozoologica* **55:** 221–229.

Fiz-Palacios O, **Leander BS**, **Heger TJ. 2014.** Old lineages in a new ecosystem: diversification of arcellinid amoebae (amoebozoa) and peatland mosses. *PLoS One* **9:** e95238.

Folmer O, **Black M**, **Hoeh W**, **Lutz R**, **Vrijenhoek R. 1994.** DNA primers for amplification of mitochondrial cytochrome c oxidase subunit I from diverse metazoan invertebrates. *Molecular Marine Biology and Biotechnology* **3:** 294–299.

Fournier B, **Malysheva E**, **Mazei Y**, **Moretti M**, **Mitchell EAD. 2012.** Toward the use of testate amoeba functional traits as indicator of floodplain restoration success. *European Journal of Soil Biology* **49:** 85–91.

Fournier B, **Lara E**, **Jassey VEJ**, **Mitchell EAD. 2015.** Functional traits as a new approach for interpreting testate amoeba palaeo-records in peatlands and assessing the causes and consequences of past changes in species composition. *Holocene* **25:** 1375–1383.

Giribet G, **Edgecombe GD**, **Wheeler WC**, **Babbitt C. 2002.** Phylogeny and systematic position of opiliones: a combined analysis of chelicerate relationships using morphological and molecular data. *Cladistics* **18:** 5–70.

Gilbert D, **Mitchell EAD**, **Amblard C**, **Bourdier G**, **Francez AJ. 2003.** Population dynamics and food preferences of the testate amoeba *Nebela tincta major-bohemica-collaris* complex (Protozoa) in a *Sphagnum* peatland. *Acta Protozoologica* **42:** 99–104.

Gomaa F, **Todorov M**, **Heger TJ**, **Mitchell EAD**, **Lara E. 2012.** SSU rRNA phylogeny of Arcellinida (Amoebozoa) reveals that the largest arcellinid genus, *Difflugia* Leclerc 1815, is not monophyletic. *Protist* **163:** 389–399.

Gomaa F, **Yang J**, **Mitchell EAD**, **Zhang WJ**, **Yu Z**, **Todorov M**, **Lara E. 2015.** Morphological and molecular diversification of Asian endemic *Difflugia tuberspinifera* (Amoebozoa, Arcellinida): a case of fast morphological evolution in protists? *Protist* **166:** 122–130.

Gomaa F, **Lahr DJG**, **Todorov M**, **Li J**, **Lara E. 2017.** A contribution to the phylogeny of agglutinating Arcellinida (Amoebozoa) based on SSU rRNA gene sequences. *European Journal of Protistology* **59:** 99–107.

Gomes e Souza MB. 2021. *Tecamebas*. Available at: https://www.tecamebas.com.br/ (accessed 15 March 2021).

Greef R. 1866. Ueber einige in der Erde lebende Amöben und andere Rhizopoden. *Archiv für Mikroskopische Anatomie* **2:** 299–331.

Grospietsch T. 1954. Studien über die Rhizopodenfauna von Schweidisch Lappland. *Archiv für Hydrobiologie* **49:** 546–580.

Hebert PDN, **Ratnasingham S**, **DeWaard JR. 2003.** Barcoding animal life: cytochrome c oxidase subunit 1 divergences among closely related species. *Proceedings of the Royal Society B: Biological Sciences* **270:** S96–S99.

Heger TJ, **Pawlowski J**, **Lara E**, **Leander BS**, **Todorov M**, **Golemansky V**, **Mitchell EAD. 2011.** Comparing potential *COI* and SSU rDNA barcodes for assessing the diversity and phylogenetic relationships of cyphoderiid testate amoebae (Rhizaria: Euglyphida). *Protist* **162:** 131–141.

Heger TJ, **Mitchell EAD**, **Leander BS. 2013.** Holarctic phylogeography of the testate amoeba *Hyalosphenia papilio* (Amoebozoa: Arcellinida) reveals extensive genetic diversity explained more by environment than dispersal limitation. *Molecular Ecology* **22:** 5172–5184.

Hegner RW. 1920. The relations between nuclear number, chromatin mass, cytoplasmic mass, and shell characteristics in four pieces of the genus *Arcella*. *Journal of Experimental Zoology* **30:** 1–95.

Huelsenbeck JP, **Ronquist F. 2001.** MRBAYES: Bayesian inference of phylogenetic trees. *Bioinformatics* **17:** 754–755.

Huelsenbeck JP, **Larget B**, **Alfaro ME. 2004.** Bayesian phylogenetic model selection using reversible jump Markov chain Monte Carlo. *Molecular Biology and Evolution* **21:** 1123–1133.

ICZN. **1999.** *International Code of Zoological Nomenclature (ICZN)*. London: International Commission on Zoological Nomenclature.

Inoue K, **Harris JL**, **Robertson CR**, **Johnson NA**, **Randklev CR. 2020.** A comprehensive approach uncovers hidden diversity in freshwater mussels (Bivalvia: Unionidae) with the description of a novel species. *Cladistics* **36:** 88–113.

Kalyaanamoorthy S, **Minh BQ**, **Wong T**, **von Haeseler A**, **Jermiin LS. 2017.** ModelFinder: fast model selection for accurate phylogenetic estimates. *Nature Methods* **14:** 587–589.

Katoh K, **Misawa K**, **Kuma KI**, **Miyata T. 2002.** MAFFT: a novel method for rapid multiple sequence alignment based on fast Fourier transform. *Nucleic Acids Research* **30:** 3059–3066.

Kent WS. 1880–1881. *A manual of the Infusoria: including a description of all known flagellate, ciliate, and tentaculiferous Protozoa, British and foreign, and an account of the organization and affinities of the sponges, Vol. 1.* London: D. Bogue, 1–472.

Koenig I, **Christinat K**, **D'inverno M**, **Mitchell EAD. 2018.** Impact of two hot and dry summers on the community structure and functional diversity of testate amoebae in an artificial bog, illustrating their use as bioindicators of peatland health. *Mires and Peat* **21:** 1–24.

Kosakyan A, **Lara E. 2019.** Using testate amoebae communities to evaluate environmental stress: a molecular biology perspective. In: *Encyclopedia of environmental health*. Dordrecht: Elsevier, 308–313.

Kosakyan A, **Heger TJ**, **Leander BS**, **Todorov M**, **Mitchell EAD**, **Lara E. 2012.** *COI* barcoding of nebelid testate amoebae (Amoebozoa: Arcellinida): extensive cryptic diversity and redefinition of the Hyalospheniidae Schultze. *Protist* **163:** 415–434.

Kosakyan A, **Gomaa F**, **Mitchell EAD**, **Heger TJ**, **Lara E. 2013.** Using DNA-barcoding for sorting out protist species complexes: a case study of the *Nebela tincta–collaris–bohemica* group (Amoebozoa; Arcellinida, Hyalospheniidae). *European Journal of Protistology* **49:** 222–237.

Kosakyan A, **Gomaa F**, **Lara E**, **Lahr DJG. 2016a.** Current and future perspectives on the systematics, taxonomy and nomenclature of testate amoebae. *European Journal of Protistology* **55:** 105–117.

Kosakyan A, **Lahr DJG**, **Mulot M**, **Meisterfeld R**, **Mitchell EAD**, **Lara E. 2016b**. Phylogenetic reconstruction based on *COI* reshuffles the taxonomy of hyalosphenid shelled (testate) amoebae and reveals the convoluted evolution of shell plate shapes. *Cladistics* **32:** 606–623.

Kostka M, **Lares-Jiménez LF**, **Tyml T**, **Dyková I. 2017.** *Copromyxa laresi* n. sp. (Amoebozoa: Tubulinea) and transfer of *Cashia limacoides* (Page, 1967) to *Copromyxa* Zopf, 1885. *Journal of Eukaryotic Microbiology* **64:** 173–182.

Kudryavtsev A, **Pawlowski J**, **Hausmann K. 2009.** Description and phylogenetic relationships of *Spumochlamys perforata* n. sp. and *Spumochlamys bryora* n. sp. (Amoebozoa, Arcellinida). *Journal of Eukaryotic Microbiology* **56:** 495–503.

Lahr DJG, **Lara E**, **Mitchell EAD. 2012.** Time to regulate microbial eukaryote nomenclature. *Biological Journal of the Linnean Society* **107:** 469–476.

Lahr DJG, **Grant JR**, **Katz LA. 2013.** Multigene phylogenetic reconstruction of the Tubulinea (Amoebozoa) corroborates four of the six major lineages, while additionally revealing that shell composition does not predict phylogeny in the Arcellinida. *Protist* **164:** 323–339.

Lahr DJG, **Kosakyan A**, **Lara E**, **Mitchell EAD**, **Morais L**, **Porfirio-Sousa AL**, **Ribeiro GM**, **Tice AK**, **Pánek T**, **Kang S**, **Brown MW. 2019.** Phylogenomics and morphological reconstruction of Arcellinida testate amoebae highlight diversity of microbial eukaryotes in the Neoproterozoic. *Current Biology* **29:** 991–1001.

Lamentowicz M, **Kajukało-Drygalska K**, **Kołaczek P**, **Jassey VEJ**, **Gąbka M**, **Karpińska-Kołaczek M. 2020.** Testate amoebae taxonomy and trait diversity are coupled along an openness and wetness gradient in pine-dominated Baltic bogs. *European Journal of Protistology* **73:** 125674.

Lansac-Tôha F, **Velho L**, **Costa D**, **Simões N**, **Alves G. 2014.** Structure of the testate amoebae community in different habitats in a neotropical floodplain. *Brazilian Journal of Biology* **74:** 181–190.

Lara E, **Heger TJ**, **Ekelund F**, **Lamentowicz M**, **Mitchell EAD. 2008.** Ribosomal RNA genes challenge the monophyly of the Hyalospheniidae (Amoebozoa: Arcellinida). *Protist* **159:** 165–176.

Lara E, **Dumack K**, **García-Martín JM**, **Kudryavtsev A**, **Kosakyan A. 2020.** Amoeboid protist systematics: a report on the 'Systematics of amoeboid protists' symposium at the VIIIth ECOP/ISOP meeting in Rome, 2019. *European Journal of Protistology* **76:** 125727.

Larget B, **Simon DL. 1999.** Markov chain Monte Carlo algorithms for the Bayesian analysis of phylogenetic trees. *Molecular Biology and Evolution* **16:** 750–759.

Larson A. 1998. The comparison of morphological and molecular data in phylogenetic systematics. In: DeSalle R, Schierwater B, eds. *Molecular approaches to ecology and evolution*. Basel: Birkhäuser.

Leidy J. 1874. Notice of some new fresh-water rhizopods. *Proceedings of the Academy of Natural Sciences of Philadelphia 3rd Series* **26:** 77–79.

Leidy J. 1876. Remarks on Arcella, etc. *Proceedings of the Academy of Natural Sciences of Philadelphia* **3:** 28.

Leidy J. 1879. Fresh-water rhizopods of North America. *Report of the United States Geological Survey of the Territories* **12:** 1–324.

Maddison WP. 1997. Gene trees in species trees. *Systematic Biology* **46:** 523–536.

Maggi, L. 1888. Sur les Protozoaires vivant sur les mousses des plantes. *Archivio Italiano di Biologia* **10:** 184–189.

Mahé F, **De Vargas C**, **Bass D**, **Czech L**, **Stamatakis A**, **Lara E**, **Singer D**, **Mayor J**, **Bunge J**, **Sernaker S**, **Siemensmeyer T**, **Trautmann I**, **Romac S**, **Berney C**, **Kozlov A**, **Mitchell EAD**, **Seppey CVW**, **Egge E**, **Lentendu G**, **Wirth R**, **Trueba G**, **Dunthorn M. 2017.** Parasites dominate hyperdiverse soil protist communities in Neotropical rainforests. *Nature Ecology and Evolution* **1:** 1–8.

Marcisz K, **Jassey VEJ**, **Kosakyan A**, **Krashevska V**, **Lahr DJG**, **Lara E**, **Lamentowicz Ł**, **Lamentowicz M**, **Macumber A**, **Mazei Y**, **Mitchell EAD**, **Nasser NA**, **Patterson RT**, **Roe HM**, **Singer D**, **Tsyganov AN**, **Fournier B. 2020.** Testate amoeba functional traits and their use in paleoecology. *Frontiers in Ecology and Evolution* **8**. Doi:10.3389/fevo.2020.575966.

Marshall KLA, **Philpot KE**, **Stevens M. 2016.** Microhabitat choice in island lizards enhances camouflage against avian predators. *Scientific Reports* **6:** 1–10.

Martin TE. 1998. Are microhabitat preferences of coexisting species under selection and adaptive? *Ecology* **79:** 656–670.

Mas-Peinado P, **Buckley D**, **Ruiz JL**, **García-París M. 2018.** Recurrent diversification patterns and taxonomic complexity in morphologically conservative ancient lineages of *Pimelia* (Coleoptera: Tenebrionidae). *Systematic Entomology* **43:** 522–548.

Mayden RL. 1997. A hierarchy of species concepts: the denouement in the saga of the species problem. In: Claridge MF, Dawah HA, Wilson MR, eds. *Species: the units of diversity*. London: Chapman & Hall.

Mayr E. 1944. *Systematics and the origin of species, from the viewpoint of a zoologist*. New York: Columbia University Press.

Medioli FS, **Scott DB**, **Abbott BH. 1987.** A case study of protozoan intraclonal variability: taxonomic implications. *Journal of Foraminiferal Research* **17:** 28–47.

Meisterfeld R. 1991. Vertical distribution of Difflugia hydrostatica (Protozoa, Rhizopoda). *Internationale Vereinigung für Theoretische und Angewandte Limnologie: Verhandlungen* **24:** 2726–2728.

Mignot JP, **Raïkov IB. 1992.** Evidence for meiosis in the testate amoeba *Arcella*. *Journal of Protozoology* **39:** 287–289.

Miller MA, **Pfeiffer W**, **Schwartz T. 2010.** *Creating the CIPRES Science Gateway for inference of large phylogenetic trees*. New Orleans: 2010 Gateway Computing Environments Workshop (GCE). IEEE, 1–8.

Mitchell EAD, **Charman DJ**, **Warner BG. 2008.** Testate amoebae analysis in ecological and paleoecological studies of wetlands: past, present and future. *Biodiversity and Conservation* **17:** 2115–2137.

Mori E, **Menchetti M**, **Zozzoli R**, **Milanesi P. 2019.** The importance of taxonomy in species distribution models at a global scale: the case of an overlooked alien squirrel facing taxonomic revision. *Journal of Zoology* **307:** 43–52.

Nasser NA, **Patterson RT**, **Roe HM**, **Galloway JM**, **Falck H**, **Sanei H. 2020.** Use of Arcellinida (testate lobose amoebae) arsenic tolerance limits as a novel tool for biomonitoring arsenic contamination in lakes. *Ecological Indicators* **113:** 106177.

Nassonova E, **Smirnov A**, **Fahrni J**, **Pawlowski J. 2010.** Barcoding amoebae: comparison of SSU, ITS and COI genes as tools for molecular identification of naked lobose amoebae. *Protist* **161:** 102–115.

Nguyen LT, **Schmidt HA**, **Von Haeseler A**, **Minh BQ. 2015.** IQ-TREE: a fast and effective stochastic algorithm for estimating maximum-likelihood phylogenies. *Molecular Biology and Evolution* **32:** 268–274.

Nguyen-Viet H, **Bernard N**, **Mitchell EAD**, **Cortet J**, **Badot PM**, **Gilbert D. 2007.** Relationship between testate amoeba (protist) communities and atmospheric heavy;metals accumulated in *Barbula indica* (Bryophyta) in Vietnam. *Microbial Ecology* **53:** 53–65.

Nikolaev SI, **Mitchell EAD**, **Petrov NB**, **Berney C**, **Fahrni J**, **Pawlowski J. 2005.** The testate lobose amoebae (order Arcellinida Kent, 1880) finally find their home within amoebozoa. *Protist* **156:** 191–202.

Nixon KC, **Wheeler QD. 1990.** An amplification of the phylogenetic species concept. *Cladistics* **6:** 211–223.

Novenko EY, **Tsyganov AN**, **Volkova EM**, **Kupriyanov DA**, **Mironenko I V.**, **Babeshko K V.**, **Utkina AS**, **Popov V**, **Mazei YA. 2016.** Mid- and Late Holocene vegetation dynamics and fire history in the boreal forest of European Russia: a case study from Meshchera lowlands.

Palaeogeography, Palaeoclimatology, Palaeoecology **459:** 570–584.

Ogden CG. 1979. Siliceous structures secreted by members of the subclass Lobosia (Rhizopodea: Protozoa). *Bulletin of the British Museum [Natural History]. Zoology* **36:** 203–207.

Ogden CG. 1991. Gas vacuoles and flotation in the testate amoeba *Arcella discoides*. *Journal of Protozoology* **38:** 269–270.

Ogden CG, **Meisterfeld R. 1989.** The taxonomy and systematics of some species of *Cucurbitella*, *Difflugia* and *Netzelia* (Protozoa: Rhizopoda); with an evaluation of diagnostic characters. *European Journal of Protistology* **25:** 109–128.

Padial JM, **Miralles A**, **De la Riva I**, **Vences M. 2010.** The integrative future of taxonomy. *Frontiers in Zoology* **7:**1–14.

Patterson RT, **Lamoureux EDR**, **Neville LA**, **Macumber AL. 2013.** Arcellacea (testate lobose amoebae) as pH indicators in a pyrite mine-acidified lake, northeastern Ontario, Canada. *Microbial Ecology* **65:** 541–554.

Penard E. 1890. Études sur les Rhizopodes d'eau douce. *Mémoires dela Société de physique et d'histoire naturelle de Genève* **31:** 1–230.

Penard E. 1902. *Faune rhizopodique du bassin du Léman.* Genéve: Henry Kündig.

Perty M. 1852. *Zur Kenntniss kleinster Lebensformen nach Bau, Funktionen, Systematik, mit Spezialverzeichniss der in der Schweiz beobachteten.* Bern: Jent und Reinert.

Playfair GI. 1918. Rhhizopods of Sydney and Lismore. *Proceedings ofthe Linnean Society of New South Wales* **42:** 633–675.

Porfírio-Sousa AL, **Ribeiro GM**, **Lahr DJG. 2017.** Morphometric and genetic analysis of *Arcella intermedia* and *Arcella intermedia laevis* (Amoebozoa, Arcellinida) illuminate phenotypic plasticity in microbial eukaryotes. *European Journal of Protistology* **58:** 187–194.

Qin Y, **Mitchell EAD**, **Lamentowicz M**, **Payne RJ**, **Lara E**, **Gu Y**, **Huang X**, **Wang H. 2013.** Ecology of testate amoebae in peatlands of central China and development of a transfer function for paleohydrological reconstruction. *Journal of Paleolimnology* **50:** 319–330.

de Queiroz K, **Donoghue MJ. 1988.** Phylogenetic systematics and the species problem. *Cladistics* **4:** 317–338.

R Core Team. **2013.** *R: a language and environment for statistical computing.* Vienna: R Foundation for Statistical Computing. Available at: http://www.R-project.org/. Accessed May 2020.

Rambaut A. 2012. *FigTree, molecular evolution, phylogenetics and epidemiology, v.1.4.* Edinburgh: University of Edinburgh, Institute of Evolutionary Biology. Available at: http://tree.bio.ed.ac.uk/software/Figtree. Accessed May 2020.

Rambaut A, **Drummond AJ**, **Xie D**, **Baele G, Suchard MA. 2018.** Posterior summarization in Bayesian phylogenetics using Tracer 1.7. *Systematic Biology* **67:** 901–904.

Reczuga MK, **Swindles GT**, **Grewling Ł**, **Lamentowicz M. 2015.** *Arcella peruviana* sp. nov. (Amoebozoa: Arcellinida, Arcellidae), a new species from a tropical peatland in Amazonia. *European Journal of Protistology* **51:** 437–449.

Roe HM, **Patterson RT. 2014.** Arcellacea (testate amoebae) as bio-indicators of road salt contamination in lakes. *Microbial Ecology* **68:** 299–313.

Ronquist F, **Teslenko M**, **Van Der Mark P**, **Ayres DL**, **Darling A**, **Höhna S**, **Larget B**, **Liu L**, **Suchard MA**, **Huelsenbeck JP. 2012.** MrBayes 3.2: efficient Bayesian phylogenetic inference and model choice across a large model space. *Systematic Biology* **61:** 539–542.

Rstudio T. 2020. *RStudio: integrated development for R.* Boston: Rstudio Team, PBC. Available at: http://www.rstudio.com/. Accessed May 2020.

Schaudinn. **1898.** Rhizopoda Ost-Afrikas. In: Reimer D, ed. *Die Thierwelt Deutsch Ostafrikas und der Nachbargebiete. Wirbellose Thiere.* Berlin: Reimer.

Schlegel M, **Meisterfeld R. 2003.** The species problem in protozoa revisited. *European Journal of Protistology* **39:** 349–355.

Schneider CA, **Rasband WS**, **Eliceiri KW. 2012.** NIH Image to ImageJ: 25 years of image analysis. *Nature Methods* **9:** 671–675.

Schönborn W. 1962. Neue Testaceen aus dem Grossen Stechlinsee und dessen Umgebung. *Limnologica* **1:** 83–91.

Schwind LTF, **Arrieira RL**, **Dias JD**, **Simões NR**, **Bonecker CC**, **Lansac-Tôha FA. 2016.** The structure of planktonic communities of testate amoebae (Arcellinida and Uglyphida) in three environments of the Upper Paraná River basin, Brazil. *Journal of Limnology* **75:** 78–89.

Siemensma FJ. 2019. *Microworld, world of amoeboid organisms.* Available at: https://www.arcella.nl/ (accessed 10 November 2020).

Singer D, **Kosakyan A**, **Pillonel A**, **Mitchell EAD**, **Lara E. 2015.** Eight species in the *Nebela collaris* complex: *Nebela gimlii* (Arcellinida, Hyalospheniidae), a new species described from a Swiss raised bog. *European Journal of Protistology* **51:** 79–85.

Singer D, **Kosakyan A**, **Seppey CVW**, **Pillonel A**, **Fernández LD**, **Fontaneto D**, **Mitchell EAD**, **Lara E. 2018.** Environmental filtering and phylogenetic clustering correlate with the distribution patterns of cryptic protist species. *Ecology* **99:** 904–914.

Singer D, **Mitchell EAD**, **Payne RJ**, **Blandenier Q**, **Duckert C**, **Fernández LD**, **Fournier B**, **Hernández CE**, **Granath G**, **Rydin H**, **Bragazza L**, **Koronatova NG**, **Goia I**, **Harris LI**, **Kajukało K**, **Kosakyan A**, **Lamentowicz M**, **Kosykh NP**, **Vellak K**, **Lara E. 2019.** Dispersal limitations and historical factors determine the biogeography of specialized terrestrial protists. *Molecular Ecology* **28:** 3089–3100.

Smith HG, **Wilkinson DM. 2007.** Not all free-living microorganisms have cosmopolitan distributions – The case of *Nebela* (*Apodera*) *vas* Certes (Protozoa: Amoebozoa: Arcellinida). *Journal of Biogeography* **34:** 1822–1831.

Swofford DL. 2002. *PAUP* phylogenetic analysis using parsimony* (and other methods), v.4.0.* Sunderland: Sinauer Associates.

Todorov M, **Bankov N. 2019.** *An atlas of Sphagnum-dwelling testate amoebae in Bulgaria.* Bulgaria: Pensoft Publishers.

Tsyganov A, **Mazei Y. 2006.** Morphology and biometry of *Arcella intermedia* (Deflandre, 1928) comb. nov. from Russia

and a review of hemispheric species of the genus *Arcella* (Testcealobosea, Arcellinida). *Protistology* **4:** 361–369.

Tsyganov AN, **Shatilovich A V.**, **Esaulov AS**, **Chernyshov VA**, **Mazei NG**, **Malysheva EA**, **Mazei YA. 2017.** Morphology and phylogeny of the testate amoebae *Euglypha bryophila* Brown, 1911 and *Euglypha cristata* Leidy, 1874 (Rhizaria, Euglyphida). *European Journal of Protistology* **61:** 76–84.

Van Oye P. 1926. Six rhizopodes nouveau du Congo belge. *Archives de Zoologie Expérimentale et Générale* **65**: Notes et Rev. 64–74.

Van Oye P. 1941. Die Rhizopoden des Sphagnetums bei Krisuvik auf Island. *Biologisch Jaarboek, Antwerpen* **7:** 284–305.

de Vargas C, **Audic S**, **Henry N**, **Decelle J**, **Mahé F**, **Logares R**, **Lara E**, **Berney Ć**, **Le Bescot N**, **Probert I**, **Carmichael M**, **Poulain J**, **Romac S**, **Colin S**, **Aury JM**, **Bittner L**, **Chaffron S**, **Dunthorn M**, **Engelen S**, **Flegontova O**, **Guidi L**, **Horák A**, **Jaillon O**, **Lima-Mendez G**, **Lukeš J**, **Malviya S**, **Morard R**, **Mulot M**, **Scalco E**, **Siano R**, **Vincent F**, **Zingone A**, **Dimier C**, **Picheral M**, **Searson S**, **Kandels-Lewis S**, **Acinas SG**, **Bork P**, **Bowler C**, **Gorsky G**, **Grimsley N**, **Hingamp P**, **Iudicone D**, **Not F**, **Ogata H**, **Pesant S**, **Raes J**, **Sieracki ME**, **Speich S**, **Stemmann L**, **Sunagawa S**, **Weissenbach J**, **Wincker P**, **Karsenti E**, **Boss E**, **Follows M**, **Karp-Boss L**, **Krzic U**, **Reynaud EG**, **Sardet C**, **Sullivan MB**, **Velayoudon D. 2015.** Eukaryotic plankton diversity in the sunlit ocean. *Science* **348:** 6237.

Velho LFM, **Lansac-Tôha FA**, **Bini LM. 2003.** Influence of environmental heterogeneity on the structure of testate amoebae (Protozoa, Rhizopoda) assemblages in the plankton of the Upper Paraná River floodplain, Brazil. *International Review of Hydrobiology* **88:** 154–166.

Venables WN, **Ripley BD. 2002.** *Modern applied statistics with S (fourth)*. New York: Springer. Available at: http://www.stats.ox.ac.uk/pub/MASS4. Accessed May 2020.

Wailes GH. 1913. Freshwater Rhizopoda from North and South America. *Journal of the Linnean Society of London, Zoology* **32:** 201–218.

Wheeler QD, **Meier R. 2000.** *Species concepts and phylogenetic theory: a debate*. New York: Columbia University Press.

Wickham H. 2016. *Ggplot2 elegant graphics for data analysis (Use R! series)*. New York: Springer.

Wiley EO. 1978. The evolutionary species concept reconsidered. *Systematic Zoology* **27:** 17–26.

Wilson EO. 2017. Biodiversity research requires more boots on the ground: comment. *Nature Ecology and Evolution* **1:** 1590–1591.

Wright K. 2017. *Corrgram: plot a correlogram, v.1.12*. Available at: https://cran.r-project.org/web/packages/corrgram/. Accessed May 2020.

Xia Y, **Gu HF**, **Peng R**, **Chen Q**, **Zheng YC**, **Murphy RW**, **Zeng XM. 2012.** *COI* is better than 16S rRNA for DNA barcoding Asiatic salamanders (Amphibia: Caudata: Hynobiidae). *Molecular Ecology Resources* **2:** 48–56.

Zhao CF, **Wei R**, **Zhang XC**, **Xiang QP. 2020.** Backbone phylogeny of *Lepisorus* (Polypodiaceae) and a novel infrageneric classification based on the total evidence from plastid and morphological data. *Cladistics* **36:** 235–258.

Zrzavý J, **Mihulka S**, **Kepka P**, **Bezděk A**, **Tietz D. 1998.** Phylogeny of the Metazoa based on morphological and 18S ribosomal DNA evidence. *Cladistics* **14:** 249–285.

SUPPORTING INFORMATION

Additional Supporting Information may be found in the online version of this article at the publisher's web-site.

Table S1. Measurements of the cells used for the morphometric analyses. Variables: test length, test width, aperture length, aperture width, mean diameter (test mean) and mean aperture.
Table S2. Coefficients of linear discriminants functions 1 (LD1) and 2 (LD2).
Table S3. Key to the new species.
Figure S1. Distance table and a neighbour-joining tree (minimum evolution criterion) of 52 *COI* sequences.
Figure S2. A, a frequency boxplot representing the original habitat on the x-axis and the different sections after Deflandre (1928) on the y-axis. B, scatterplot of the scores of linear discriminants with x-axis representing discriminant function 1 (LD1) and y-axis representing discriminant function 2 (LD2). Colours and symbols represent the original habitats where the organisms were collected: freshwater (blue), *Sphagnum* (red) and terrestrial mosses (green); the table represents the prediction accuracy. C, scatterplot of the scores of linear discriminants, the colours and symbol represent the different sections after Deflandre (1928) Section 1 'Vulgares' (orange squares), Section 2 'Carinatae' (red circles) and Section 3 'Aplanatae' (pink triangles); the table represents the prediction accuracy.
Figure S3. Image comparing the new species described: *Arcella guadarramensis*, *Galeripora balari, Galeripora bufonipellita*, *Galeripora galeriformis*, *Galeripora naiadis, Galeripora sitiens* and *Galeripora succelli*. Representing scanning electron micrographs of the oral (A), aboral (B), detail of the test (C) and light microscopic images (D), with a scale.
Appendix S1. Synonymic list of infraorders Sphaerothecina.